UNIVERSITAT POLITÈCNICA DE VALÈNCIA

_ TELECOM ESCUELA TÉCNICA VLC SUPERIOR DE INGENIERÍA DE TELECOMUNICACIÓN

UNIVERSITAT POLITÈCNICA DE VALÈNCIA

School of Telecommunications Engineering

Performance Analysis of NB-IoT Using Link Level Simulations.

Master's Thesis

Master's Degree in Telecommunication Engineering

AUTHOR: Tutunovic , Marija

Tutor: Gómez Barquero, David

External cotutor: CESANA, MATTEO

Experimental director: AVELLAN CARRION, CRISTINA

ACADEMIC YEAR: 2021/2022

Acknowledgements

I would like to express my deepest gratitude to prof. Gomez-Barquero for giving me the opportunity to work on this topic at the iTEAM, for all of his invaluable advice, suggestions and feedback, support and inspiration. Many thanks to UPV and ETSIT for their generous support.

This endeavor would not have been possible without Jaime, whose patience and persistence have been the foundation that held this work together. I am also very grateful for Cristina and all the hard work and time she has put in, even though not everything was included in the final version. I had the pleasure of working with amazing people at iTEAM and I am grateful to all of them for their support, their hospitality, how easily they had accepted me into their team and the efforts they made to overcome the language barrier together.

I am deeply indebted to all of my friends for believing in me throughout this process. Without their tremendous understanding and encouragement, especially in the past few months, it would have been impossible for me to complete this work.

Lastly, I would like to say a massive **hvala** to my family. Their belief in me and their unconditional support have kept my spirits and motivation high during this process.

Resumen

A medida que crece el interés en las aplicaciones de área amplia de baja potencia (del inglés *Low Power Wide Area*, LPWA), las tecnologías celulares ganan especial atención como posibles soluciones frente a la saturación de espectro no licenciado. En el Release 13 (Rel-13) el 3GPP define, entre su oferta de soluciones, el Internet de las Cosas de Banda Estrecha, del inglés *Narrow-Band IoT* (NB-IoT), como una tecnología celular basada en LTE que proporciona conectividad masiva de dispositivos con bajo consumo de energía, amplia cobertura y bajo coste. En las siguientes versiones, las mejoras de NB-IoT se esfuerzan por cumplir con los requisitos de *Massive Machine Type Communications* (mMTC) de la quinta generación (5G) de comunicaciones móviles. Para comprender las características de la capa física de NB-IoT, este trabajo se basa en construir un simulador NB-IoT del canal físico compartido del enlace descendente (NPDSCH) y analizar su rendimiento al usar diferentes modelos de canal, repeticiones, modos de operación y esquemas de modulación y codificación.

Abstract

As the interest in Low Power Wide Area (LPWA) applications grows, the cellular technologies gain more attention as possible solutions to the overcrowded unlicensed spectrum. In its Release 13 (Rel-13) 3GPP defines, among the solutions, Narrowband Internet of Things (NB-IoT) as an LTE-based cellular technology which provides mass connectivity of devices with low power consumption, broad coverage and low cost. Following further releases, NB-IoT enhancements strive to meet the requirements of 5^{th} Generation's (5G) Massive Machine Type Communications (mMTC). In order to understand the physical layer characteristics, this work was based on building a NB-IoT simulator of the Narrowband Physical Downlink Shared Channel (NPDSCH) and analysing the performance while using different channel models and parameters, repetitions, operation modes and Modulation and Coding Schemes (MCSs).

Contents

List of Figures

List of Tables

Lists of Acronyms

16QAM	16 Quadrature Amplitude Modulation
3GPP	3^{rd} Generation Partnership Project
5G	5^{th} Generation
ANR	Automatic Neighbor Relations
AWGN	Additive White Gaussian Noise
BER	Bit Error Rate
BLER	Block Error Rate
C-IoT	Cellular Internet of Things
CAT-NB1	Category 1 of NB-IoT
CAT-NB2	Category 2 of NB-IoT
CP	Control Plane
CP	Cyclic Prefix
CRC	Cyclic Redundancy Check
CRS	Cell Specific Reference Signal
DMRS	Demodulation Reference Signal
DRX	Discontinuous Reception
DS	Delay Spread
EC-GSM-IoT	Extended Coverage Global System for Mobile communications in the context of IoT
EDT	Earliest Data Transmission
EGPRS	Enhanced General Packet Radio Services
FDD	Frequency Division Duplexing

GNSS Global Navigation Satellite System

GSM Global System for Mobile communications

HARQ Hybrid Automatic Repeat Request

HD-FDD Half-Duplex Frequency Division Duplexing

ISI Inter Symbolic Interference

ITU International Telecommunications Union

IoT Internet of Things

LLS Link Level Simulator

LOS Line of Sight

LPWA Low Power Wide Area

LTE-M Long Term Evolution for Machines

LTE Long Term Evolution

MBMS Multimedia Broadcast and Multicast Service

MCG Mobile Communication Group

MCS Modulation and Coding Scheme

MIB Master Information Block

MIMO Multiple Input Multiple Output

MRC Maximum-ration Combining

NB-IoT Narrowband Internet of Things

NGSO Non-Geosynchronous Orbit

NLOS Non Line of Sight

NPBCH Narrowband Physical Broadcast Channel

NPDCCH Narrowband Physical Downlink Control Channel

NPDSCH Narrowband Physical Downlink Shared Channel

NPRACH Narrowband Physical Random Access Channel

NPRS Narrowband Positioning Refernce Signal

NPSS Narrowband Primary Synchronisation Signal

NPUSCH Narrowband Physical Uplink Shared Channel

NRS Narrowband Reference Signal

NR New Radio

NSSS Narrowband Secondary Synchronisation Signal

NTN Non-Terrestrial Networks

NWUS Narrowband Wake Up Signal

OFDM Orthogonal Frequency Division Multiplexing

PRB Physical Resource Block

PSM Power Saving Mode

PUR Preconfigured Uplink Resources

QPSK Quadrature phase-Shift Keying

QoS IQuality of Service

RAI Release Assistance Indication

RA Random Access

RE Resource Element

RRC Radio Resource Control

RU Resource Unit

SC-FDMA Single Carrier Frequency Division Multiple Access

SC-PTM Single-Cell Point to Multipoint

SCS Subcarrier Spacing

SFN System Frame Number

SF Subframe

SON Self-Organizing Network

SR Scheduling Request

TBS Transport Block Size

TDD Time Division Duplexing

TDL Tapped Delay Channel Model

UE	User Equipment
UL	Uplink
UPV	Universitat Politècnica de València
UP	User Plane
URLLC	Ultra-reliable and low latency communications
VoLTE	Voice over LTE
WUS	Wake-Up Signal
eDRX	Extended Discontinuous Reception
eMBB	Enhanced Mobile Broadband
iTEAM	Telecommunications and Multimedia Applications Research Institute
mMTC	Massive Machine Type Communications

Chapter 1

Introduction and objectives

1.1 Introduction

With each new decade, the International Telecommunications Union (ITU) poses more advanced and stringent requirements for the next generation of cellular communication systems. As a cellular technology, Narrowband Internet of Things (NB-IoT) can be defined as a LPWA solution that is able to operate in licensed spectrum bands for Long Term Evolution (LTE) or as a stand-alone solution using the freed spectrum previously occupied by Global System for Mobile communications (GSM) carriers. It is designed to connect a massive number of devices, with very low cost of connectivity and low power consumption, characterized by infrequent data transmissions, while providing very good coverage, even in extreme cases. Some use cases that can leverage NB-IoT connectivity include, for instance, smart cities, smart metering or smart agriculture (waste management, detectors, parking control, low-end sensors, etc.). [1] Even though NB-IoT is LTE-based, the technology has evolved through the 3GPP releases in order to meet the requirements of 5G systems further embracing the interconnection with the IoT systems. In an overall description of NB-IoT, it can be said it is a technology designed to exploit the heterogeneity and big data processing of IoT by using high capabilities offered through the current mobile communication networks.

The idea behind NB-IoT is to develop a radio technology standard which is able to reuse the same hardware facilities and share frequency spectrum resources in perfect harmony with the existing i.e., currently deployed cellular technologies. Depending on the state of the hardware, some updates might be necessary in order to support NB-IoT, however, in case of relatively new equipment established in a station, NB-IoT may only require a software update. From the business point of view, it enables the mobile network operators to be competititive in the market of IoT. As far as the physical layer is concerned, NB-IoT completely follows the LTE model, with some minor changes discussed in more detail in Chapter 4.

1.2 Objectives

This Master's Thesis will analyze the performance of the NB-IoT physical (PHY) layer using Link Level Simulations (LLS). A comprehensive set of results obtained from a number of simulated NB-IoT subframes will be assessed depending on several network parameters. These parameters include, for example, the Modulation and Coding Scheme (MCS), the operation mode, the delay spread and the number of repetitions. This work uses MATLAB as a tool to design and develop the link-level PHY layer simulator with special focus on the user plane. Therefore, milestones of this work to achieve the overall objective are *(i)* to understand the NB-IoT technology from a theoretical and practical point of view, i.e., the concept, evolution and development through 3GPP releases, and to get familiar with the state-of-the-art of this technology, *(ii)* to develop the simulation tool using MATLAB, *(iii)* to conduct performance simulations of the NB-IoT PHY layer on the user plane, *(iv)* to analyze and draw conclusions from the results obtained. The results will focus on the typical metrics of interest such as the Block Error Rate (BLER) and the Carrier-to-Noise Ratio (CNR).

1.3 Structure of the document

This document is organized in chapters, divided into sections and subsections as detailed below:

- Chapter 2: defines the methodology used to develop and compose this work, including a detailed explanation on how the project has been managed, a list of tasks and milestones as well as the project timeline.
- Chapter 3: encapsulates the significance of NB-IoT in the modern-day scenario. A comparison between similar IoT solutions is offered, arriving to the proper definition of NB-IoT and its capabilities. The subsections of each release explore the 3GPP recommendations with their enhancements and modifications regarding the physical layer of NB-IoT and some interesting improvements regarding the standard as a whole.
- Chapter 4: offers a detailed review of the physical layer, covering different aspects and providing the necessary information needed to better understand the behavior of the system such as the operation modes, duplexing, frame structure, transmission modes, MCSs, physical channels and signals regarding both the uplink and the downlink. The understanding of the NB-IoT fundamentals is the key point to putting them into practice in the MATLAB simulator.
- Chapter 5: introduces the MATLAB simulator providing all the information regarding the implementation of the standard inside the simulator and a thorough analysis of the results obtained through the link level simulations.
- Chapter 6: contains the conclusion of the work with a summary of the important results obtained in the previous chapter and briefly proposes some future action points.

Chapter 2

Methodology

2.1 Project Development and Management

This work has been developed in collaboration with the Mobile Communication Group (MCG) of the Telecommunications and Multimedia Applications Research Institute (iTEAM) at the Universitat Politècnica de València (UPV).

The development of this project can be split into three different phases. The first phase consisted in understanding the context of the NB-IoT technology from a high-level perspective to the more practical implementation. At this point, all efforts were made to learn the role and technical requirements of NB-IoT in the modern-day scenario towards the 5G mMTC. Also, the work focused on acquiring knowledge about the NB-IoT PHY layer functionalities that would be later implemented in the MATLAB simulator. This corresponds with Chapter 3 and 4 of this document.

The second phase of the project was related to the use of MATLAB as the main simulation tool. This part of the work consisted in getting familiar with the tool, examining the current functionalities already available in the simulator, and adapting it accordingly to the NB-IoT standard specifications. Moreover, this included creating new functionalities and putting new parameters and performance conditions in place. All of the needed information is compiled in Chapter 5.

Finally, the third phase of the project was devoted to generating results that would allow the performance analysis of the NB-IoT PHY layer. Parameters such as channel model conditions, repetitions, operation modes and MCS have been introduced for generating those results (see Chapter 5). The information provided by the simulator based on those parameters has been interpreted and carefully assessed and weighted up to draw a firm conclusion regarding the chosen technology. Conclusions and future action lines can be found in Chapter 6.

2.2 Task identification

A number of tasks were identified to develop this project. The list of tasks is as follows:

1. Learn the context and the state-of-the-art of NB-IoT as a LPWA cellular technology and search for references and sources of information.
2. Study the NB-IoT physical layer from technical reports and specifications provided by major standardization bodies, namely, the 3GPP.
3. Adapt and develop new features of the MATLAB simulator to implement a NB-IoT user-plane PHY layer simulator.
4. Launch simulations for a number of different conditions, i.e., channel models, repetitions, operation modes and MCSs.
5. Process the data and manage the generated results.
6. Derive conclusions and propose future work guidelines.
7. Compose the report of this work using LaTeX.

2.3 Timeline

This work started in October 2021 when I was introduced to the Mobile Communication Group of the iTEAM Research Institute. November and December where devoted to the development of the first phase of the project. Phase 2 started during March 2022 and developed until mid-May while tasks related to phase 3 were completed during June, covering the beginning of July.

The list of tasks presented above is addressed in Table 2.1 according to the following timeline:

Table 2.1: Timeline.

Task	*October*	*November*	*December*	*March*	*April*	*May*	*June*	*July*
1	X X X	X						
2		X X X	X X X X					
3				X X	X X	X		
4					X	X X X	X	
5							X X	
6							X X	X
7							X	X

Chapter 3

State of the Art

The idea of connecting virtually anything with everything found its realization in the Internet of Things (IoT) concept. Its main hypothesis is that every device is connected, with the ability to send and receive data. When dealing with the question what it is that can be defined as anything or everything, nowadays we can get many answers. So many that, following Ericsson's example, it is possible to distinguish between four main segments of IoT depending on the characteristics and requirements of the communication devices, as shown in Figure 3.1.

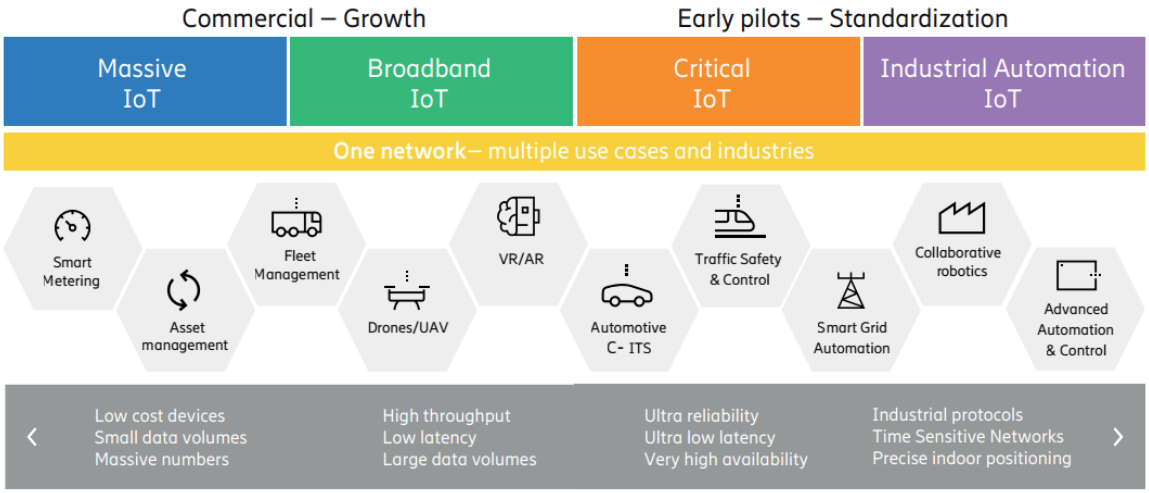

Figure 3.1: IoT main segments. (Source:[2])

These segments are defined as follows:

- **Massive IoT** covers devices characterized with long battery life, low cost and complexity, tolerance to delay and with extended coverage.
- **Broadband IoT** covers devices and vehicles with long battery life and extended coverage, but in comparison with Massive IoT, it provides much higher data rates and lower latencies that can

be seen in mobile broadband services.

- **Critical IoT** takes it a step further with extremely low latencies and ultra-high reliability at different data rates, enabling use cases in intelligent transportation systems, remote healthcare, smart utilities, smart manufacturing, and fully immersive AR/VR.
- **Industrial Automation IoT** covers applications with extremely demanding connectivity and positioning requirements with the emphasis on security and architecture. Together with Critical IoT, it forms the key enabler for the full digitalization of Industry 4.0. [2]

The variety of characteristics of these segments roughly tells us that it is difficult to find a single technology that will be able to fulfil all of the requirements of different segments, since some can be contradictive (e.g., narrow bandwidth cannot achieve high data rates, real-time applications cannot support long sleep in power saving mode, etc.). Therefore, there are many technologies to be chosen from which offer a solution to a specific IoT application. Depending on the range and bandwidth requirements, the technologies can be divided into two mainstream categories: cellular and non-cellular IoT technologies, as illustrated in Figure 3.2. The main difference between the two is the operating frequency spectrum, that can be either licensed or unlicensed, which further dictates the *(i)* capital and operational costs, *(ii)* use of available bandwidth, *(iii)* data rates, *(iv)* effects of interference and *(v)* security. [3]

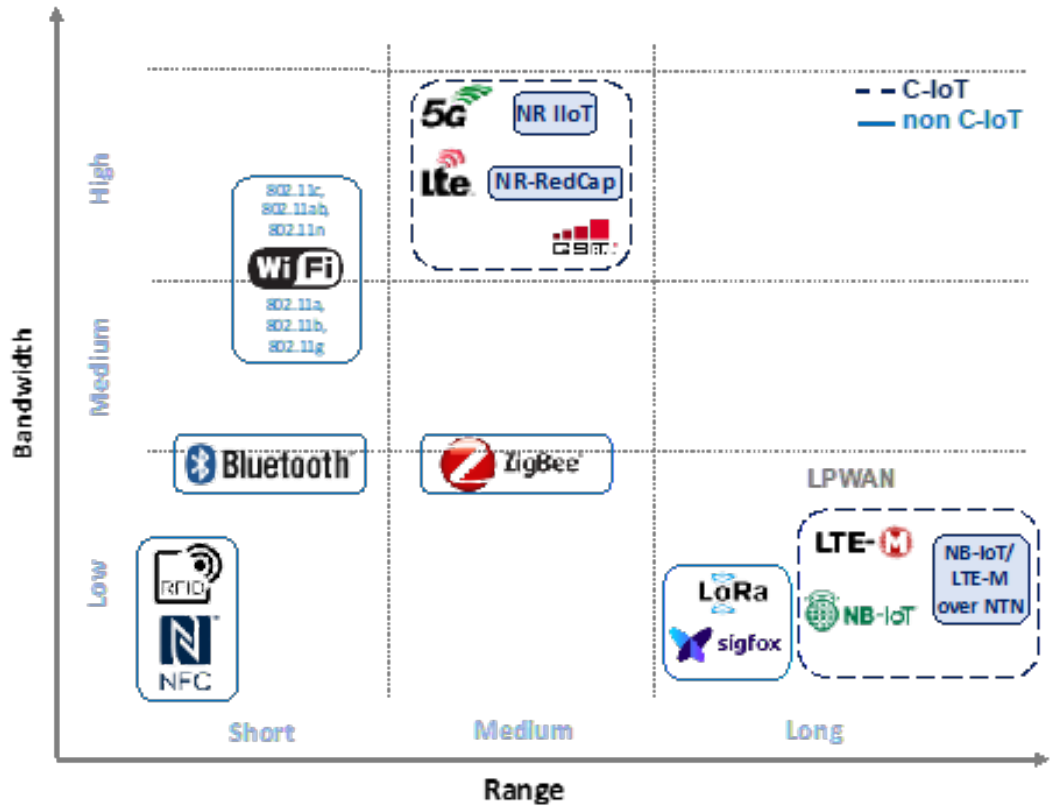

Figure 3.2: IoT technologies. (Source:[3])

Lately, a growing interest for the category of LPWA applications has been shown from both academia and industry. LPWA networks have been widely considered as the future wireless communication standard for IoT. They are characterized by long range, low power and low cost with relaxed throughput requirements, with options in both categories expanding worldwide: LoRa and SigFox as non C-IoT technologies and LTE-M and NB-IoT as C-IoT technologies. [4] As the unlicensed radio band gets more crowded, affecting the reliability and the delivered QoS, the focus has shifted onto C-IoT technologies and their benefits.

3.1 The 5G era

The ITU defined IMT-2020 to cover all mobile systems that include the new capabilities of IMT that go beyond those of IMT-Advanced. There are three usage scenarios:

- **Enhanced Mobile Broadband (eMBB)** comes with new application areas and requirements in addition to existing Mobile Broadband applications for improved performance and an increasingly seamless user experience to target high data rate applications.
- **Massive machine type communications (mMTC)** are characterized by a very large number of connected devices typically transmitting a relatively low volume of non-delay-sensitive data.
- **Ultra-reliable and low latency communications (URLLC)** have stringent requirements for throughput, latency and availability.

Some of the performance requirements of IMT-2020 include very high peak data rate, very high and guaranteed user experience data rate, quite low air interface latency, quite high mobility while providing satisfactory quality of service, enabling massive connection in very high density scenarios, very high energy efficiency for network and device side, greatly enhanced spectral efficiency, significantly larger area traffic capacity, high spectrum and bandwidth flexibility, ultra high reliability and good resilience capability, enhanced security and privacy, compared to the previous, IMT-Advanced, which is illustrated in Figure 3.3. [5]

Release 13 introduced the Extended Coverage Global System for Mobile communications in the context of IoT (EC-GSM-IoT) as an LPWA technology based on Enhanced General Packet Radio Services (EGPRS). It was designed as long range, long battery life and low complexity system which is able to coexist with the existing mobile networks. Although it has never been deployed in a real-life scenario, the main idea has been further explored within the release of LTE making 4G competitive in the field of MTC. Specifically, through LTE-M, also known as enhanced MTC (eMTC), and NB-IoT. In general, LTE-M provides richer capabilities than NB-IoT. It can support mobility, Voice over LTE (VoLTE) and higher data rates of up to 1 Mbps in comparison with NB-IoT's 30 kbps. However, NB-IoT achieves better coverage and lower power consumption. Further details of the NB-IoT features will be addressed in Chapter 4. Taking this information into account, we could say that LTE-M is more adequate for Broadband IoT, while NB-IoT satisfies the requirements for Massive IoT. Currently,

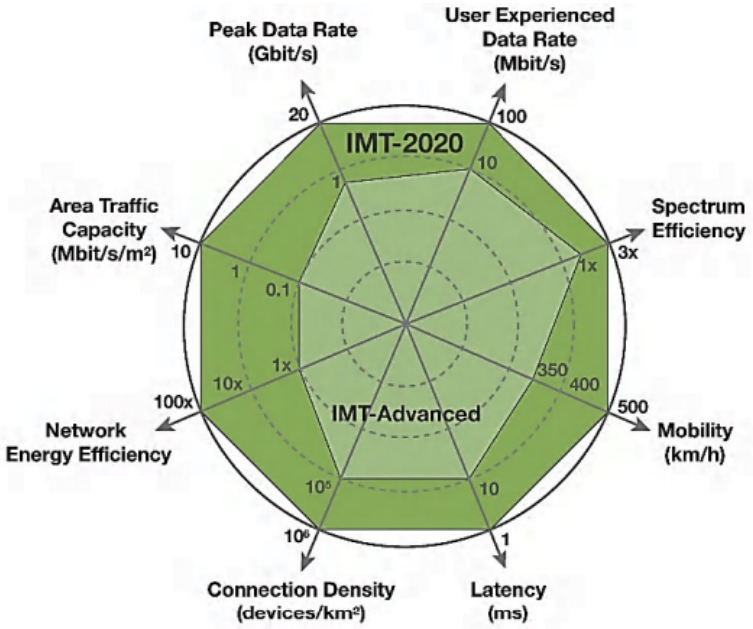

Figure 3.3: Minimum IMT-2020 requirements.(Source:[6])

mMTC continues to use 4G IoT. In the initial phase, 5G inherited the air interface standards of NB-IoT and eMTC. [3]

3.2 NB-IoT through 3GPP releases

From the previous section we come to understand that some LTE solutions still fulfil the requirements of 5G, and therefore 3GPP continues to explore their enhancements through the new releases. This is depicted graphically in the Figure 3.4. As the objective of this work is to analyze NB-IoT, it will only focus on the definitions, recommendations and enhancements of this specific technology.

3.2.1 Release 13

3GPP Rel-13 first introduced and described the architecture of NB-IoT. This will be further discussed in the following chapter. In order to optimally reduce the signalling in this C-IoT solution, the release proposes Control Plane (CP) optimization and User Plane (UP) optimization. There are only two states regarding the Radio Resource Control (RRC) modes of operation: *RRC-IDLE* and *RRC-CONNECTED*.

In case of network using CP optimization RRC connection reconfiguration and re-establishment are not supported, while in the case of UP optimization an RRC connection resume procedure is used at transition from *RRC-IDLE* to *RRC-CONNECTED* where previously stored information in the User Equipment (UE) as well as in the eNB (LTE base station) is utilised to resume the RRC connection. In the message to resume, the UE provides a Resume ID to be used by the eNB to access the stored

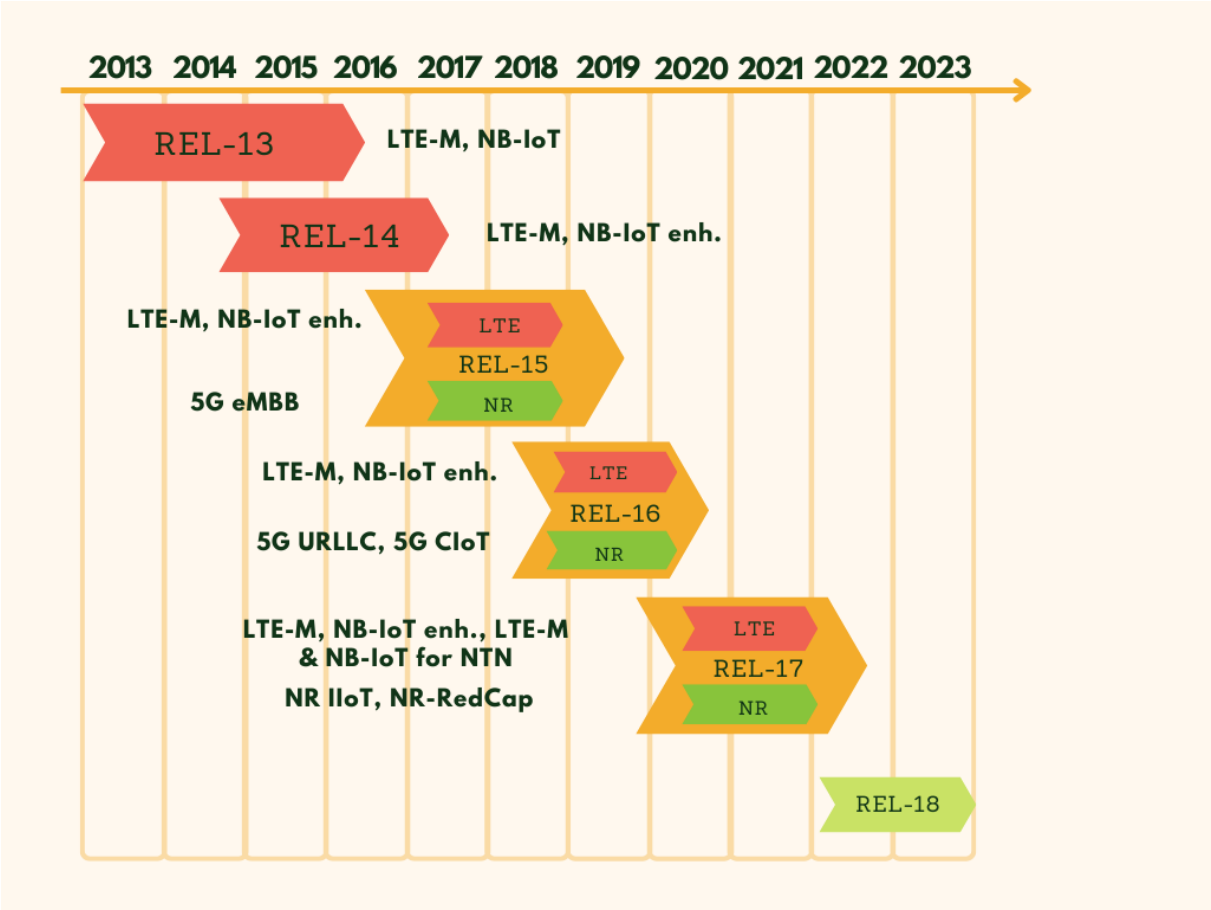

Figure 3.4: The evolution of C-IoT through 3GPP releases

information required to resume the RRC connection. The simplification of these processes allows for low complexity and low price devices.

Regarding the requirements of NB-IoT devices to have a long battery life of 10 years and more, Rel-13 introduces DRX as a power saving technique in *RRC-CONNECTED* state, while there are two mechanisms, PSM and eDRX, in *RRC-IDLE* state. [7] [8]

3.2.2 Release 14

This release contains many enhancements of Rel-13. Firstly, it supports an additional category of devices CAT-NB2, which in comparison with the previously defined user category CAT-NB1, supports larger Transport Block Size (TBS), two HARQ processes and offers higher data rates. Secondly, it introduces the Narrowband Positioning Reference Signal (NPRS) which improves the basic positioning method used previously. Since the legacy LTE Multimedia Broadcast and Multicast Service (MBMS) scheme is not suitable for NB-IoT, Rel-14 introduces multicast support through Single-Cell Point to Multipoint (SC-PTM) communication. It brought multicarrier enhancements by enabling paging and RA procedure on non-anchor carriers. Moreover, it supports Release Assistance Indication (RAI)

message used to indicate that the user has no more data to transmit, the connection can be released, and the device may go to idle state, and lower UL transmit power compared to Rel-13 which further enables smaller batteries, low device power consumption and even lower device cost. [7] [9]

3.2.3 Release 15

Further enhancements are introduced in this release, such as Earliest Data Transmission (EDT) which aims to improve the battery life of the user and reduce message latency by transmitting small data packets during RA procedure, Time Division Duplexing (TDD) which optimizes the utilization of the available spectrum with a few differences compared to the conventional LTE, Wake-Up Signal (WUS) which is used to further reduce the NB-IoT user power consumption and Scheduling Request (SR) is enabled for NB-IoT users. This release also supports Radio Link Control (RLC) Unacknowledged Mode (UM) bearers for NB-IoT, 1.25 kHz subcarrier spacing for NPRACH with the minimum hopping distance of 1.25 kHz and NB-IoT deployment in small-cell. [7] [10]

3.2.4 Release 16

This release improves EDT by introducing UL transmission using Preconfigured Uplink Resources (PUR) that enables transmission in IDLE mode without performing random access procedures. This can improve uplink transmission efficiency and reduce UE power consumption. It also adds the SON/ANR function for NB-IoT which is used for network optimization. Rel-16 improves multicarrier operations by reporting channel quality in Msg3 and connected mode, reduces latency with the support for UE specific DRX and improves mobility by providing assistance information for inter-RAT cell selection. Maybe the most important step towards NR is undertaken in this release which describes the coexistence of NB-IoT with NR and the connection of NB-IoT to 5G Core network. [7] [11]

3.2.5 Release 17

From the physical layer point of view, Rel-17 introduces 16 Quadrature Amplitude Modulation (16QAM) both in downlink and uplink. The newest feature enabled in this release is the support for NB-IoT UEs over Non-Terrestrial Networks (NTN), specifically for UEs with Global Navigation Satellite System (GNSS) capability. In order to compensate for the long propagation delays present in NTN systems, this release defines the use of either increased timer values and window sizes or delayed starting times for both the physical layer and the higher layers. In case of Non-Geosynchronous Orbit (NGSO), due to the satellite movement, periods of discontinuous coverage may manifest, therefore in order for the UE to save power, the network will provide satellite assistance information (i.e., parameters that enable the UE to calculate and predict when the following satellite will provide coverage). [12] [13]

The summary of the standard introduction and enhancements with each release is depicted in the

Figure 3.5.

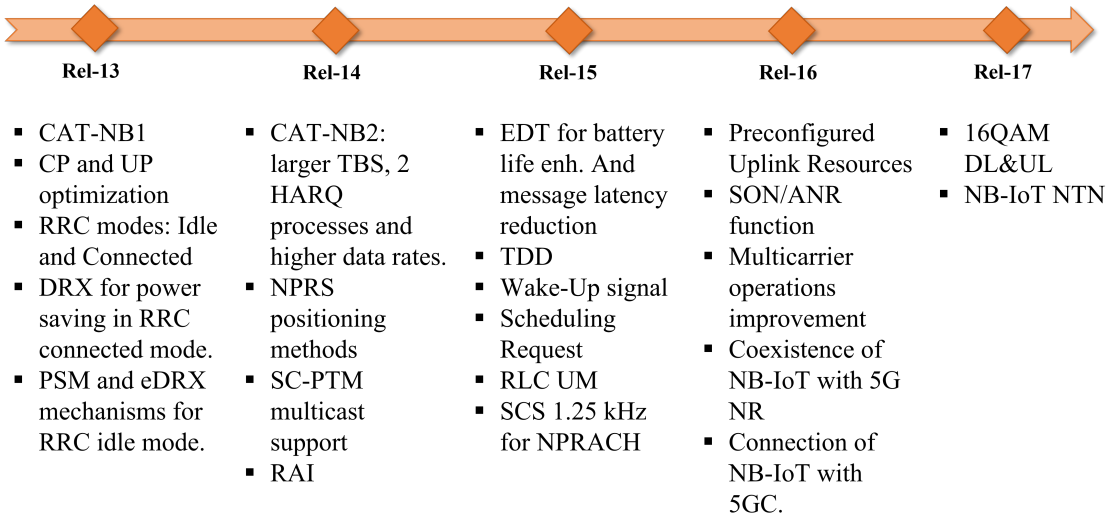

Figure 3.5: NB-IoT release evolution

Chapter 4

NB-IoT Physical Layer

NB-IoT reuses the LTE design, so unlike other IoT technologies which require the deployment of new infrastructures, NB-IoT can be easily implemented in the existing LTE infrastructure with some changes. These changes include *(i)* a fixed transmission bandwidth of 180 kHz, *(ii)* the difference in waveform generation formula of Single Carrier Frequency Division Multiple Access (SC-FDMA), *(iii)* the resource element mapping, *(iv)* the transmission pattern of synchronization signals, and *(v)* repetitive transmissions. As LTE is designed to provide data rates of up to 100 Mbps, NB-IoT has the goal of adapting it for very low throughput services that make up the most of IoT. In the Table 4.1 we summarize the most important characteristics of NB-IoT, while in the text below we focus on the parts of the PHY layer features needed for implementation inside the simulation tool.

Table 4.1: Table of summary of NB-IoT characteristics.

Transmission bandwidth	180 kHz
Range	10 km
Access scheme	OFDMA, SC-FDMA
Physical Resource Blocks (PRB)	1 PRB
Deployment scenarios	In-band, guard-band, stand-alone
Duplexing	FDD, HD-FDD (type B), TDD (Rel-15)
SCS	15 kHz (DL and UL), 3.75 kHz (UL)
Transmission modes	Single-tone, multi-tone
MCS	QPSK, 16QAM (Rel-17) Convolutional coding (DL), Turbo coding (NPUSCH)
Physical channels and signals	DL: NPBCH, NPDCCH, NPDSCH, NPSS, NSSS, NPRS, NWUS, NRS UL: NPUSCH, NPRACH, DMRS
Coverage	164 dB Max Coupling Loss (MCL), Mobility support
Number of devices	Support for massive number of devices: approx. 50,000 per cell
Battery life	Very long (10-15 years)
Complexity/Cost	Ultra-low compared tp LTE Cat-1/Cat-4 devices

4.1 Operation modes

The legacy LTE defines 6 Physical Resource Blocks (PRB) as the minimum number, and 100 PRBs as the maximum number, depending on the channel bandwidth. By reducing the minimum system bandwidth to one PRB bandwidth of the LTE, the NB-IoT can be deployed in three scenarios, i.e. in-band mode, guard-band mode, and stand-alone mode, as seen in Figure 4.1. These different operation modes allow the technology to exploit efficiently the available spectrum resources and with a certain level of flexibility.

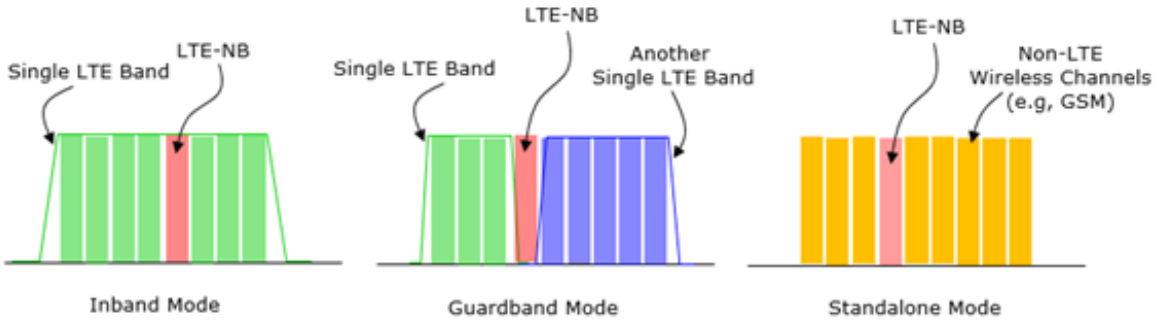

Figure 4.1: Operation modes of NB-IoT. (Source:[14])

In the case of in-band and guard-band modes, the NB-IoT signal occupies one PRB from the LTE bandwidth, thus allowing the benefits of cost savings and ease of integration. However, the in-band mode is limited to a predefined set of possible PRBs, in order to avoid conflicts with essential LTE channels and signals. The guard-band mode overcomes this restriction by using the unused resource blocks within an LTE carrier's guard-band but, only in the case of bandwidth of 5 MHz or more. In the case of stand-alone mode, the NB-IoT signal occupies the bandwidth of a carrier other than LTE, using a new frequency carrier, usually the liberated spectrum of GSM. The stand-alone mode has the additional 20 kHz used for guard band. [7] [15]

4.2 Duplexing

Initially, the transmission mode of the NB-IoT system was defined as purely frequency-division duplexing (FDD) where downlink and uplink transmissions are performed in separated frequency bands. Due to device constraints such as low complexity and long battery life, NB-IoT UE supports half-duplex FDD (HD-FDD) where the device is not able to transmit and receive information at the same time, but performs the actions one after the other [16]. Specifically, it supports half-duplex type B in which a whole subframe is used as a guard between reception and transmission [15]. From Release 15, NB-IoT also supports TDD, but with a few differences in comparison to the conventional LTE. [7]

4.3 Frame structure

The framing principle used in NB-IoT has been completely inherited from LTE, with both downlink and uplink transmissions organized into radio frames of a 10 ms duration each. As it was already mentioned, there are some differences to channel and signal mapping which will be discussed more in the next section.

The radio frames are divided into 10 subframes (SF) of 1 ms which, for downlink, are composed of 2 slots, each with a duration of 0.5 ms. In the frequency domain, this corresponds to a 15 kHz subcarrier spacing (SCS). The indexing of the radio frames is done using System Frame Number (SFN). As NB-IoT uses Orthogonal Frequency Division Multiplexing (OFDM), each slot consists of 7 OFDM symbols. The cyclic prefix (CP) of the first OFDM symbol lasts 5.2 μs, while for the remaining six symbols it lasts 4.7 μs, just like in the case of LTE. For NB-IoT, the extended CP is not supported though. As the SCS is defined at 15 kHz, there are 12 subcarriers per subframe in the 180 kHz bandwidth. This is represented in the Figure 4.2. A PRB is defined with one slot i.e., 7 OFDM symbols over 12 subcarriers, while a resource element (RE) is defined as one OFDM symbol per subcarrier. [7] [16]

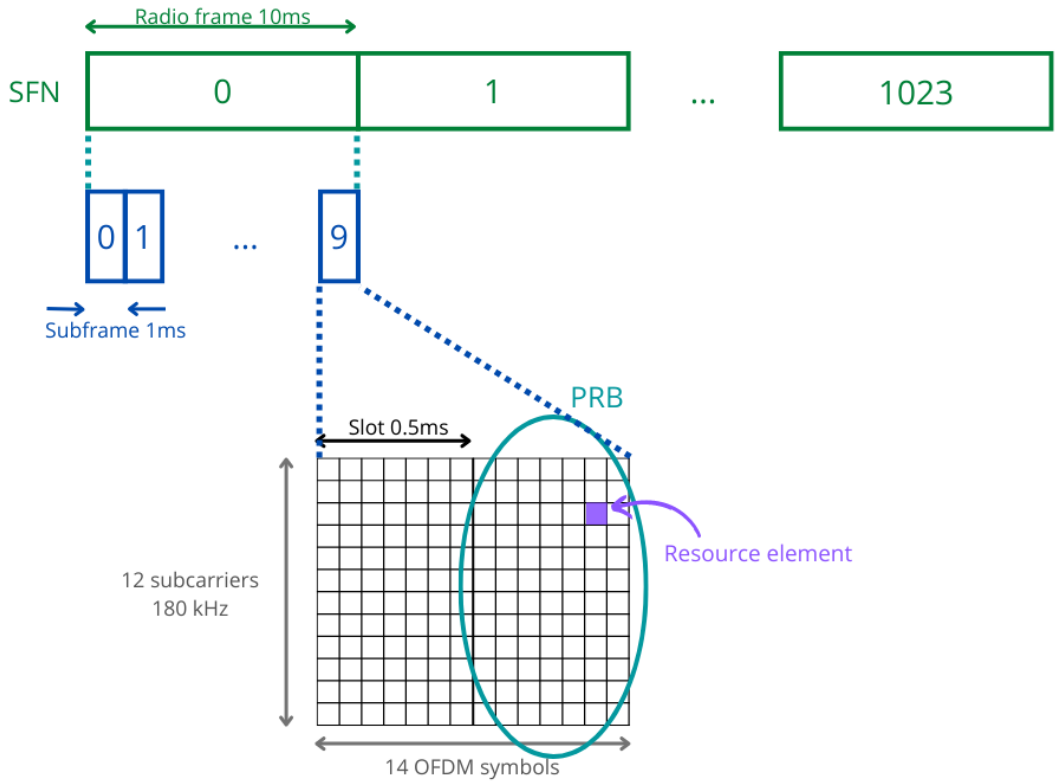

Figure 4.2: NB-IoT framing structure in downlink.

While only 15 KHz SCS is used for downlink, in the uplink there are two possible SCS formats, i.e.

Table 4.2: Frame duration

	SCS	Slot duration	Radio frame duration	Number of subcarriers	OFDM symbols per frame
Downlink	15 kHz	0.5 ms	20 slots	12	7
Uplink	15 kHz	0.5 ms	20 slots	12	7
	3.75 kHz	2 ms	5 slots	48	7

15 kHz and 3.75 kHz. For the 3.75 kHz SCS, the slot duration is 4 times longer than in the previous case i.e., it last 2 ms. Therefore, the radio frame is divided into 5 slots, each consisting of 7 OFDM symbols over 48 subcarriers, as can be seen in the Figure 4.3 and summarized in the Table 4.2.

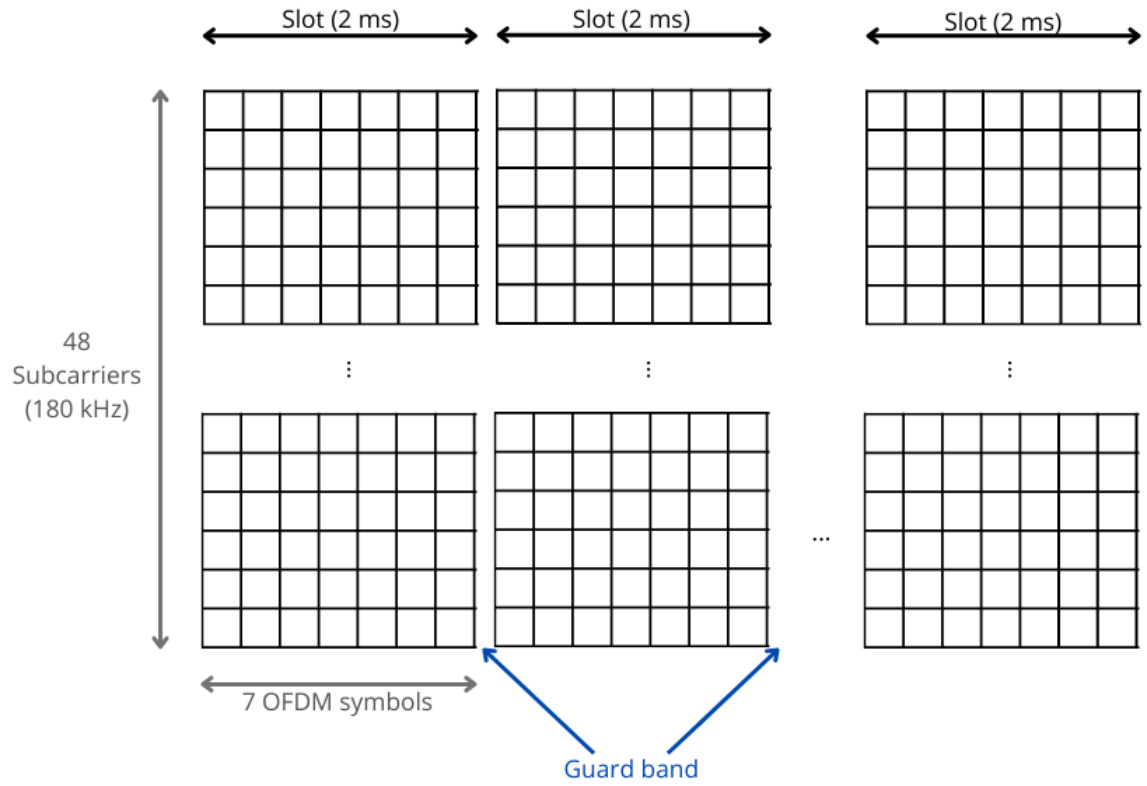

Figure 4.3: NB-IoT framing structure in uplink, 3.75 kHz SCS.

4.4 Tranmission modes

NB-IoT allows for two transmission options, single-tone and multi-tone. The multi-tone option is the only available in the case of downlink transmission where all 12 of the subcarriers are used. The uplink transmission options depend on the subcarrier spacing used. For the 3.75 kHz spacing, only one subcarrier can be used i.e., only single-tone transmission is possible. For the 15 kHz spacing, both

options can be performed by using one, three, six or all 12 subcarriers. [16] All of the options are depicted on Figure 4.4.

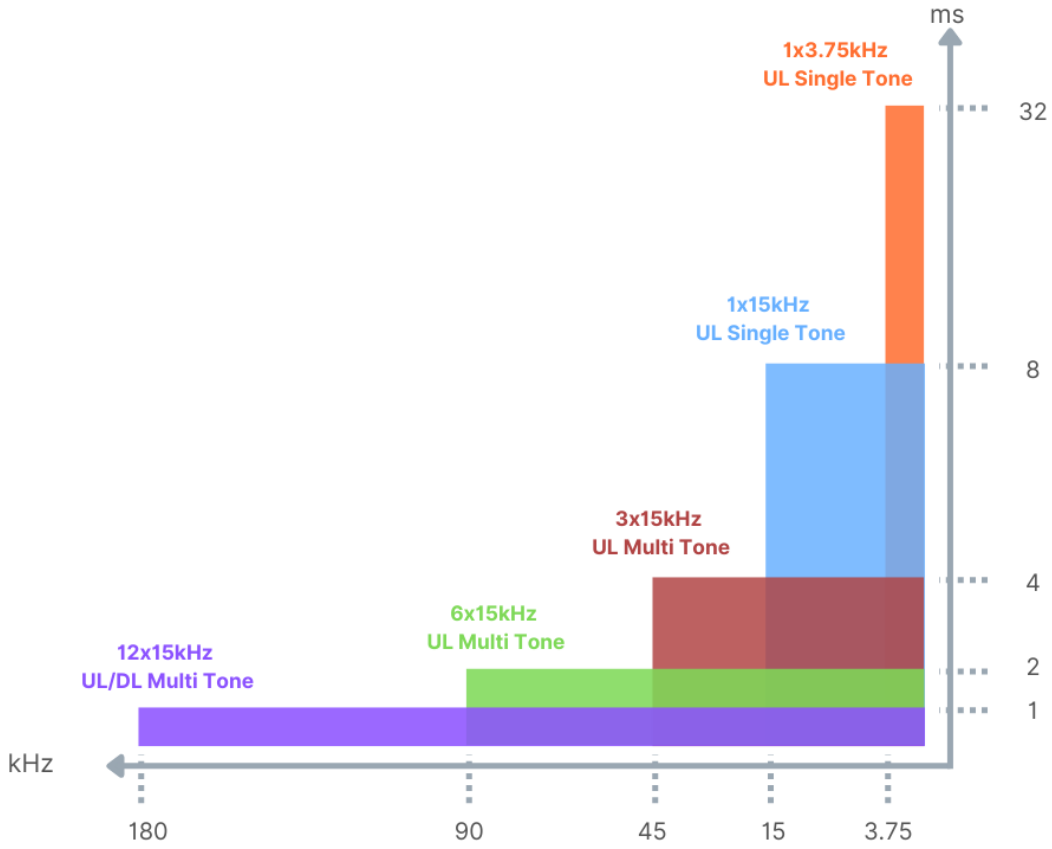

Figure 4.4: NB-IoT transmission modes.

4.5 Modulation and coding schemes

The physical downlink channels are always modulated using Quadrature Phase-Shift Keying (QPSK), therefore only 2 bits can be mapped per RE. In the uplink case, multi-tone transmission uses QPSK, while single-tone transmission uses $\pi/2$-BPSK or$\pi/4$-QPSK with phase continuity between symbols in order to reduce peak-to-average power ratio. [17] As of Rel-17, downlink shared channel and multi-tone uplink transmission support 16QAM. The TBS of each MCS is defined in the Table 4.3, following [18]. Due to the fact that the first three OFDM symbols are reserved for LTE in in-band mode, the specification defines that the MCSs which can be used in the case of QPSK are from 0 to 10, while in the case of 16QAM from 11 to 17.

In the downlink, the physical channels are coded using tail biting convolutional coding with the coding rate 1/3, while in the uplink the shared channel is coded using turbo coding with the coding rate 1/3. [19]

Table 4.3: Table of MCS and TBS.

QPSK	
MCS	TBS
0	16
1	24
2	32
3	40
4	56
5	72
6	88
7	104
8	120
9	136
10	144
11	176
12	208
13	224

16QAM	
MCS	TBS
14	256
15	280
16	296
17	336
18	376
19	408
20	440
21	488

4.6 Physical channels and signals

The number of channels and signals of the physical layer in NB-IoT is significantly reduced compared to LTE which enables low device complexity and costs. The condition of using one PRB for the transmission has led to certain modifications in the structure of the physical channels and signals, so we have newly defined standards for NB-IoT. The physical channels and signals can be classified into downlink channels and signals and uplink channels and signals, as can be seen in the Figure 4.5.

4.6.1 Downlink physical channels and signals

In the downlink we can differentiate between three physical channels: Narrowband Physical Broadcast Channel (NPBCH), Narrowband Physical Downlink Control Channel (NPDCCH) and Narrowband Physical Downlink Shared Channel (NPDSCH); and five physical signals: Narrowband Primary Synchronization Signal (NPSS), Narrowband Secondary Synchronization Signal (NSSS), Narrowband Positioning Reference Signal (NPRS), Narrowband Wake Up Signal (NWUS) and Narrowband Reference Signal (NRS).

- **NPBCH** is used to transmit the Master Information Block (MIB) and it always occupies the first subframe i.e., subframe #0 in any radio frame. Narrowband MIB is divided into 8 blocks with each block being transmitted 8 times resulting in total time of 640 ms.
- **NPDCCH** controls the data transfer between the UE and eNB, while the remaining signaling

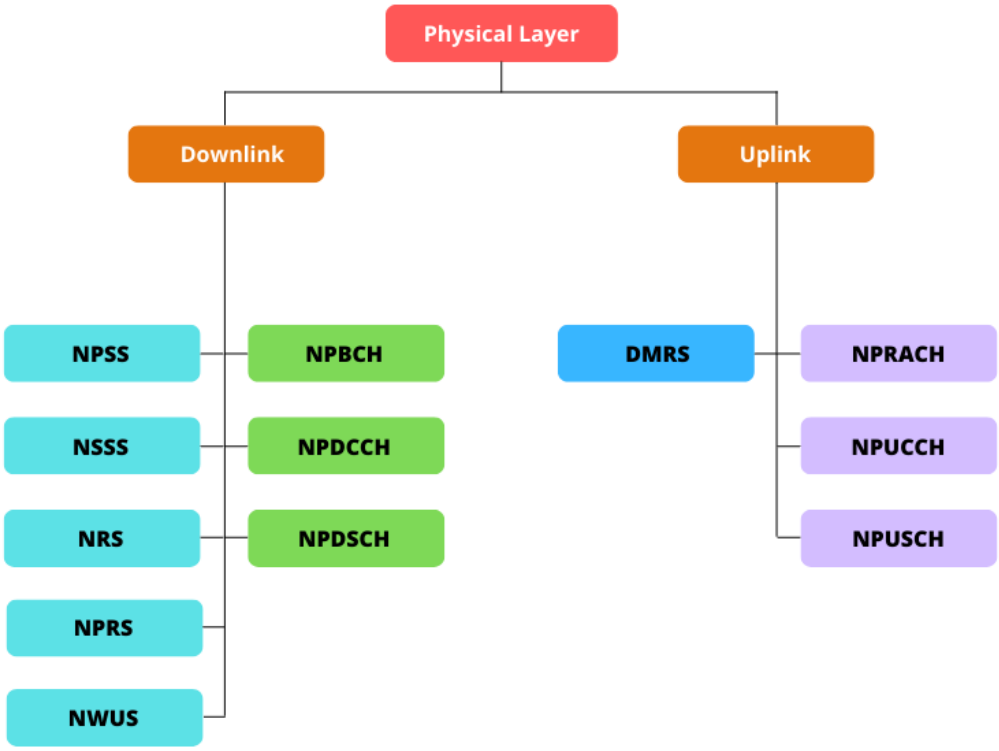

Figure 4.5: NB-IoT physical channels and signals (Rel-17).

information (paging message, system information, and RAR message) and data are transmitted over the **NPDSCH**. [7]

- **NPSS and NSSS** are used for time and frequency synchronization and cell identification. As the legacy LTE synchronization sequences occupy six PRBs, they cannot be used in the case of NB-IoT, so a new design is introduced. NPSS is transmitted in subframe #5 every 10 ms, while NSSS is transmitted in subframe #9 every 20 ms.
- **NPRS** is introduced in order to enable positioning of NB-IoT specifically.
- **NWUS** is introduced in order to reduce power consumption, as it is sent when the receiver is in idle mode.
- **NRS** is transmitted in all subframes which may be used for broadcast or dedicated downlink transmission, no matter if the actual data is transmitted or not, and it is used for channel estimation at the receiver side. As NB-IoT supports no more than two antenna ports, NRS can be transmitted on either one or both antenna ports and occupies 4 OFDM symbols per subframe per port, as shown in Figure 4.6.

In the case of the in-band operation mode, the first three OFDM symbols in each subframe are left for the eventual use by the LTE control channel, as well as all the REs dedicated to LTE cell specific

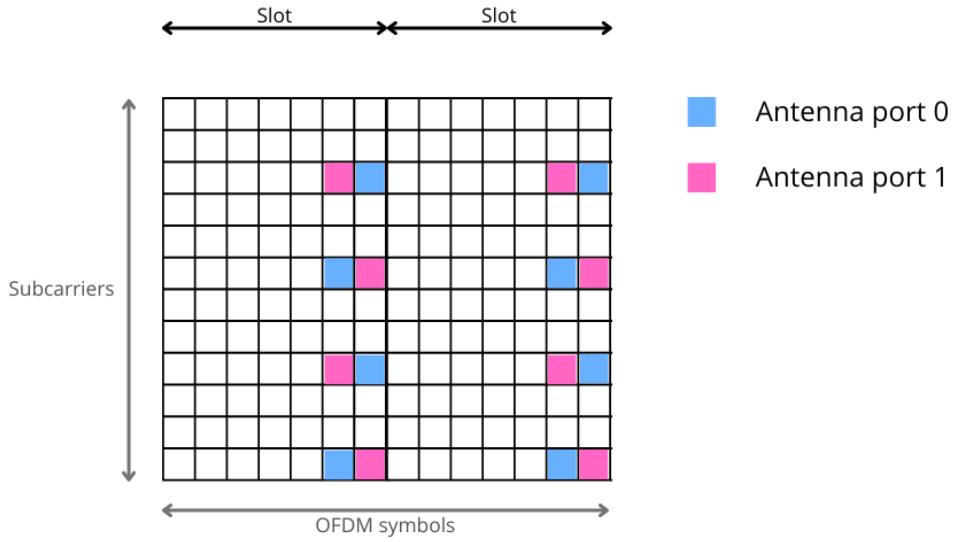

Figure 4.6: Mapping of NRS to resource elements.

reference signal (CRS). This can be seen in the Figure 4.7 as an example of using one antenna port.

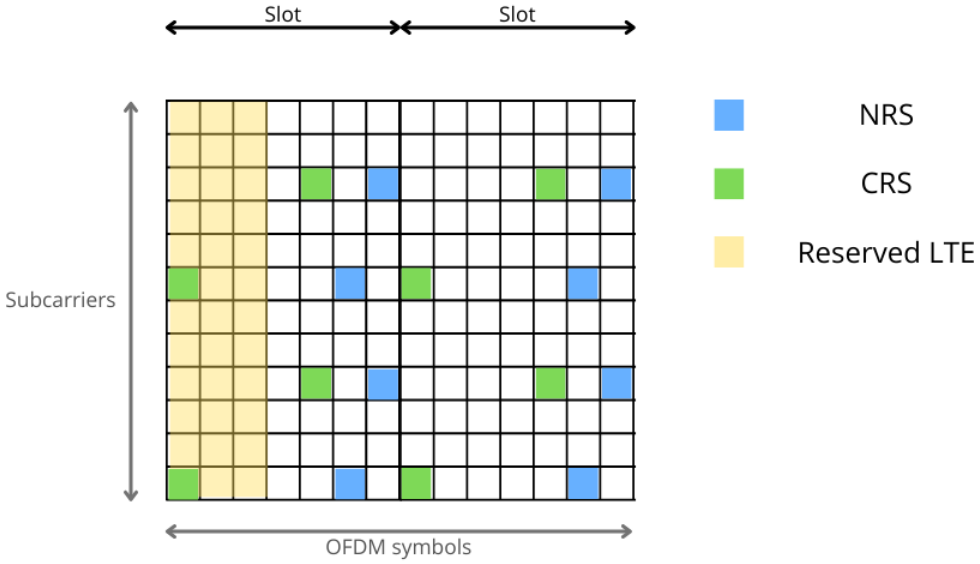

Figure 4.7: Mapping of NRS and CRS to resource elements.

In the case of the guard-band and stand-alone operation modes, since NB-IoT is completely separated from LTE, all of the OFDM symbols can be occupied by the NB-IoT signals and channels. This provides a higher throughput than in the case of in-band mode. However, due to the synchronization procedures at the receiver side the mapping of some channels and signals, such as NPBCH, NPSS and

NSSS, is defined and constant for all three operation modes. [20]

4.6.2 Uplink physical channels and signals

In the uplink we can differentiate two physical channels: Narrowband Physical Uplink Shared Channel (NPUSCH) and Narrowband Physical RandomAccess Channel (NPRACH); and one physical signal: Demodulation Reference Signal (DMRS).

- **NPUSCH** is used to transport data and control information from the UE side.
- **NPRACH** transmits the NB-IoT preamble which enables the UE to get access to the network.
- **DMRS** is used for channel estimation for uplink transmissions. The signal is mapped differently depending on the type of NPUSCH format used and the transmission mode.

Due to different transmission modes available in uplink, a resource unit (RU) is defined as the smallest unit that can be transmitted despite the SCS used. [7] [16] A single antenna port is used for all uplink transmissions. [21]

Chapter 5

MATLAB simulations

5.1 Introduction

This work centers around the implementation of a NB-IoT Link Level Simulator (LLS) inside the MATLAB environment. An LLS is a software implementation of a link between a transmitter, such as a base station, and a receiver, such as an UE, used to generate a waveform and send it over a specific type of channel model using Monte Carlo simulations that generate random channel impulse responses. Link level simulations evaluate the physical layer performance by simulating actual transmission and reception of information bits over a chosen channel involving all of the necessary signal processing blocks such as channel coding, modulation, channel estimation, etc. These simulations are important in order to validate the performance of signal processing algorithms, adjust and modify them, and ultimately test and implement new ones. Typical metrics of interest in LLS are Bit Error Rate (BER), Block Error Rate (BLER) and throughput quality metrics. It is important to emphasize that the LLS does not require any information from the higher layers (for example power control, link adaptation, HARQ, scheduling, traffic models, etc.) unlike System Level Simulators.

5.2 MATLAB Link Level Simulator

As LLS is able to evaluate the performance of the physical layer without instructions sent from the higher layers, it is assumed that the receiver and the transmitter are synchronized, i.e. we can neglect the control information passing. Hence, the focus can be put on the data information bits and the user plane which is, in this work, centered around the NPDSCH channel transmission. We assume the connection is evaluated between one transmitter and one receiver, both equipped with one antenna. The simulator scheme is depicted in the Figure 5.1.

Based on the chosen MCS and the number of subframes (in this case set to 1 per iteration), the size of the transport block is calculated and the information bits are generated. They are then sent

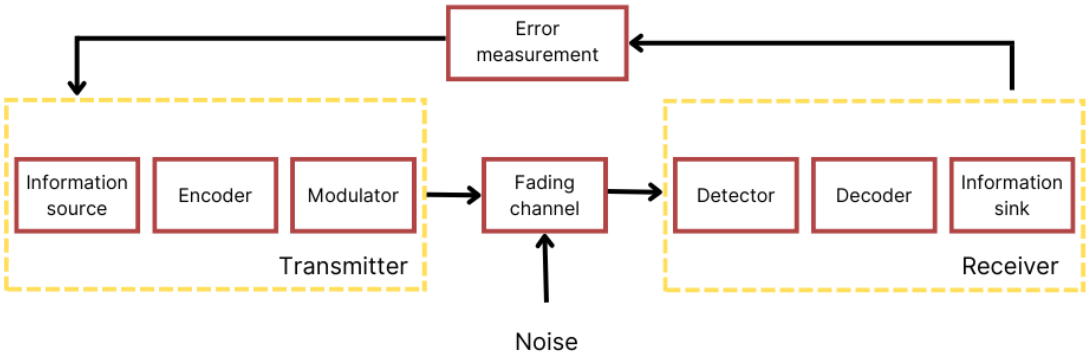

Figure 5.1: Simulator scheme.

through the Cyclic Redundancy Check (CRC), Convolutional coding, Rate matching, Scrambling and Modulation blocks. The CRC value is set to 24 bits for a NB-IoT signal. Covolutional coding was done according to the scheme in Figure 5.2, where C_k is the input bit sequence, k is the number of bits to encode, D is the number of encoded bits per output stream i, $d_k^{(i)}$ is the output bit sequence and S_i is the shift register.

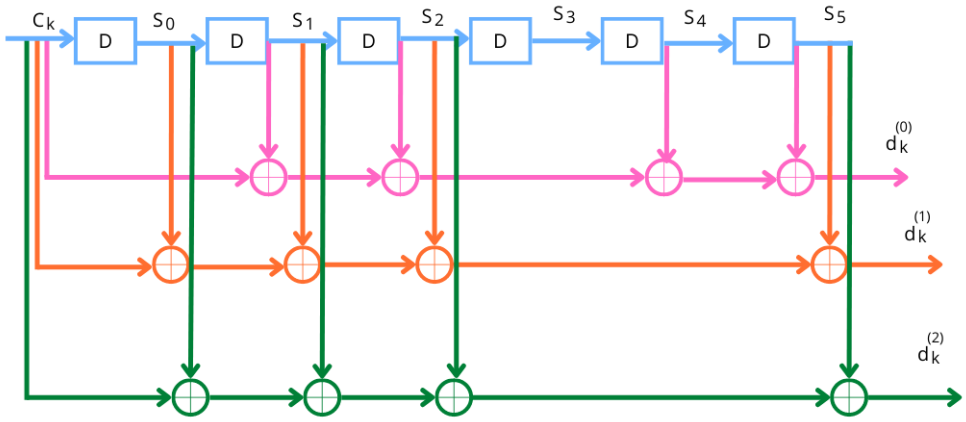

Figure 5.2: Convolutional coding scheme.

For convolutionally coded bits the rate matching process consists of interleaving the three output streams of the encoder $d_k^{(i)}$, followed by the bit collection block and the bit selection and pruning block. The process is shown on Figure 5.3 following the recommendation in [19], where $v_k^{(i)}$ is the interleaved bit sequence of $d_k^{(i)}$, w_k is the virtual circular buffer and e_k is the rate matching output bit sequence with k going from 0 to *E-1* where E is the rate matching output sequence length.

Modulation used in the simulations is QPSK. Based on this, E is set to the value of 320 bits. In the waveform generation block, NRS signals are generated following the recommendation in [13] i.e. by combining two Gold sequences (pseudo-random sequence) and mapping them to REs assuming one antenna port is used. In the case of in-band mode, CRS signals are also generated and mapped

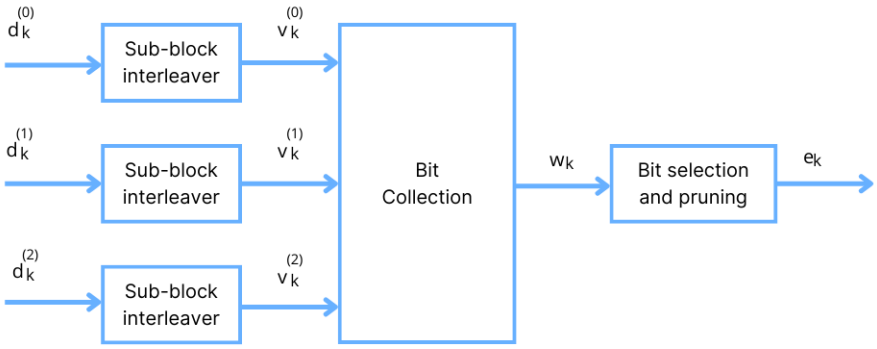

Figure 5.3: Rate matching scheme.

to the adequate REs. OFDM modulation follows, with normal CP insertion and upsampling in the case of stand-alone mode, in order to match the minimum LTE sampling rate. The signal is further sent to the channel filtering block, which encapsulates the Tapped Delay Line (TDL) channel model environment and impact, following the noise addition block. The process is depicted in the Figure 5.4.

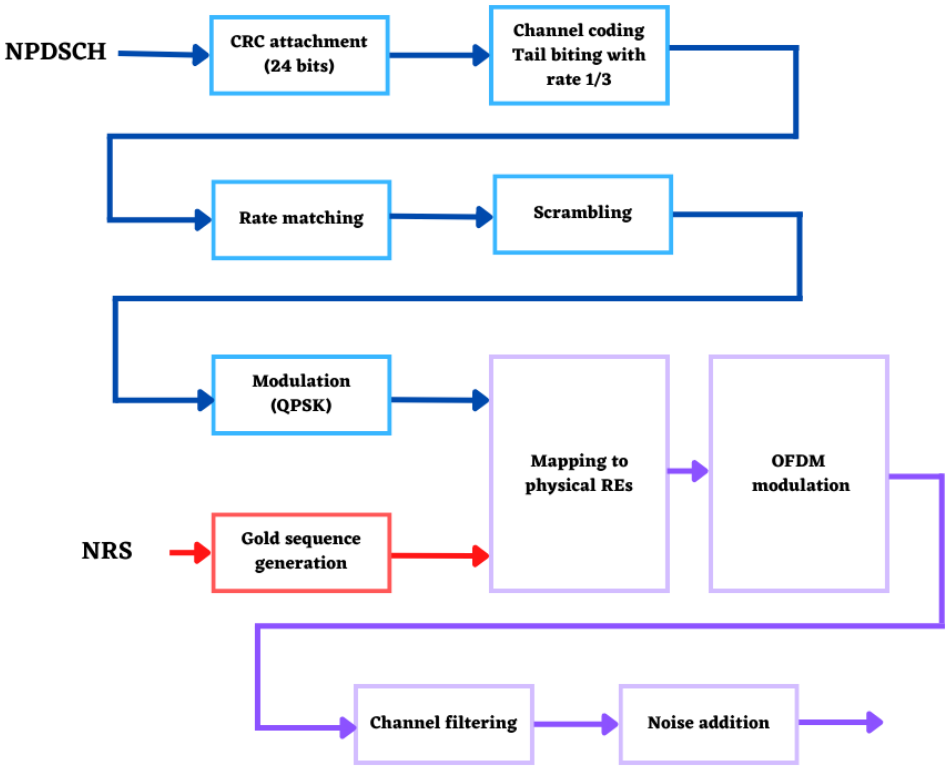

Figure 5.4: Transmission chain of the NPDSCH.

At the receiver side, the OFDM decoder block removes the CPs and, when needed, downsamples the signal. As the real estimation of the channel is implemented, the NRS (and CRS, if used) signals

Table 5.1: Number of repetitions for NPDSCH

Repetition number field	*Repetition number*
0	1
1	2
2	4
3	8
4	16
5	32
6	64
7	128
8	192
9	256
10	384
11	512
12	768
13	1024
14	1536
15	2048

are used to evaluate the effects of the channel and interpolate the values over the rest of the symbols. Using least square (LS) channel estimation method and linear interpolation first in the frequency and then in the time domain, we obtain the estimated impact of the channel on each RE. The next block uses Maximum Likelihood (ML) demapper obtaining the Log-Likelihood Ratio (LLR) metrics. Further rate recovery and decoding blocks obtain the data bits which are then compared to the originally generated bits, following the calculation of the chosen metrics. In order to improve the channel estimation procedure, [18] defines the number of repetitions according to the Table 5.1, and the procedure is implemented in the simulator. It includes the initiation of a buffer at the transmitter side which stores the originally generated bits that will be used for every repetition which includes generating a new subframe and a combiner block at the receiver side using Maximum-ration Combining (MRC) of the LLRs of each repetition transmission. The process is depicted in the Figure 5.5.

The duplexing method used in the simulator is FDD. All the simulation results have been obtained by evaluating 30,000 subframes posing as a stop condition BLER smaller than 0.1% meaning that out of 30,000 collected subframes, less than 300 have to be erroneous in order to end the simulation process. Otherwise, the CNR value is increased and the simulations are run again. In case of a repetition number larger than 1, the total number of generated subframes is 30,000 multiplied by the number of repetitions. The repetitions are combined in the combiner and regarded as if one subframe had been sent. The average time of simulating one MCS for a specific number of repetitions and DS value was around 120 hours.

Following the recommendation in [22], the channel model implemented is TDL as the most popular

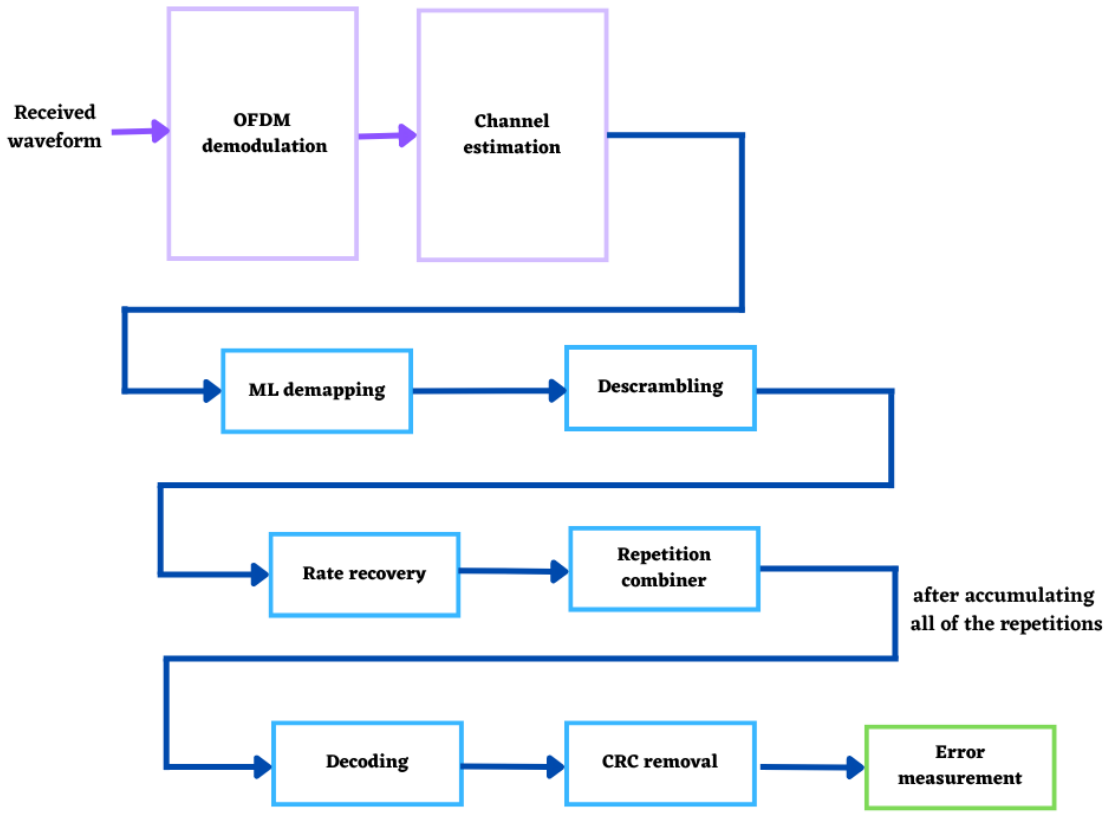

Figure 5.5: Receiver chain of the NPDSCH.

model of a multipath fading channel used for non-MIMO evaluations. Out of the five models defined in the report, first three TDL models are Non Line of Sight (NLOS) with taps characterized with a Rayleigh distribution, while the other two are Line of Sight (LOS) characterized with a Rician distribution in the first tap and a Rayleigh distribution for other taps. The main parameters defining the spectrum of each tap are the Doppler frequency and the delay spread (DS) which needs to be denormalized following the Table 5.2 from [22] for each tap considering the TDL-A model used.

The purpose of this work is to analyze the physical layer performance of NB-IoT, as it is an interesting standard designed to coexist with the current mobile communications standards. As it is a sort of simplified version of LTE, we can expect lower performance for example in the channel estimation process due to the fact that the NRS are not equally spaced through the subframe but concentrated at the REs of the last OFDM symbols in a PRB. Through the simulations we can follow the gain in CNR obtained through the repetition process, or the impact of sending more bits through the change of the order of MCS. We can also add mobility into the mix by increasing the Doppler frequency shift and change the environment of the channel.

Table 5.2: Table of frame duration

Tap #	*Normalized delay*
1	0.0000
2	0.3819
3	0.4025
4	0.5868
5	0.4610
6	0.5375
7	0.6708
8	0.5750
9	0.7618
10	1.5375
11	1.8978
12	2.2242
...	

Tap #	*Normalized delay*
...	
13	2.1718
14	2.4942
15	2.5119
16	3.0582
17	4.0810
18	4.4579
19	4.5695
20	4.7966
21	5.0066
22	5.3043
23	9.6586

5.3 Results

Since the Additive White Gaussian Noise (AWGN) channel model is the simplest channel model and reaches the stopping condition with a small number of repetitions, its results and simulations are not included in this work. Instead, the analysis will be centered around the more realistic case of the TDL channel model and a repetition number of 16 and higher. The following results are considering the case of stand-alone mode, while the parameters are defined following the Table 5.3.

Table 5.3: Table of simulation parameters

Number of subframes	30,000
CRC value	24 bits
Modulation	QPSK
Stop simulation criteria	0.1%
Channel model	TDL-A
Delay spread	10, 100, 300, 450, 1000 ns
Number of repetitions	16, 32, 64, 128

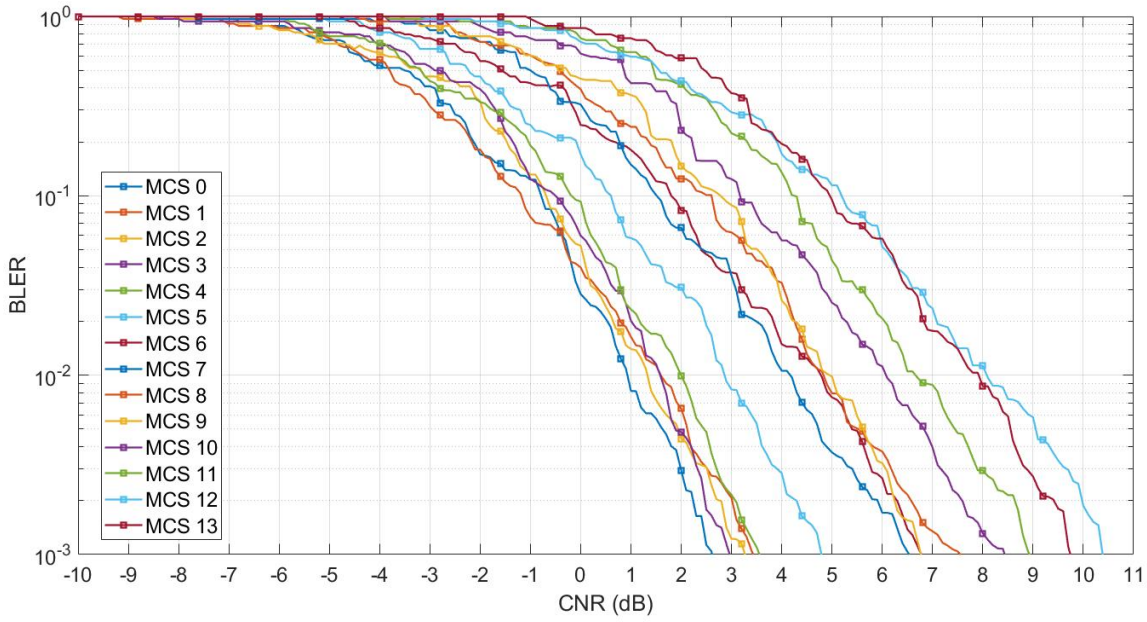

Figure 5.6: BLER v.s. CNR for 32 repetitions and DS=10ns.

In the Figure 5.6 we can see the simulation results for the case of DS set to 10 ns, Doppler frequency shift of 5 Hz and 32 repetitions for 14 MCSs, where MCS 0 can be regarded as the most robust, while MCS 13 as most efficient in terms of the bits sent. The x-axis represents the Carrier-to-Noise Ratio (CNR) in decibels (dB), while the y-axis represents the BLER values expressed in a logarithmic scale. Increasing the MCS results in higher CNR needed to obtain the same BLER. The graph shows that for a certain value of CNR, such as -2 dB, using MCS 0 we get the BLER of 17%, but in case of using

MCS 13 we get BLER of 100% meaning all of the received subframes have been erroneous and the decoding of the signal has failed. However, this degradation in signal decoding is not strictly linearly connected with the increase of the MCS.

We can notice that for certain values of CNR the curves of higher MCSs overlap and even show lower BLER values compared to MCSs with lower order. As an example, we can focus on the curve of the MCS 7 that intersects the curve of the MCS 6 five times to finally show we need to provide lower CNR values for BLER values lower than 4%. The MCS 6 curve is over-passed also by the curves of MCS 8 and MCS 9. One possible explanation for this behavior can be found in the process of rate matching, specifically, bit puncturing. Since the bits from the original sequences have been interleaved, we cannot specify exactly which ones got removed in the rate matching process and that may introduce some performance differences between all of MCSs.

This graph shows that the condition of BLER smaller than 0.1% is reached for all the MCSs with different values of CNR. The best scenario regarding the lowest CNR necessary is achieved by using the MCS 0 with CNR = 2.7 dB, while in the worst case it would be to use MCS 12 as it requires CNR = 10.4 dB.

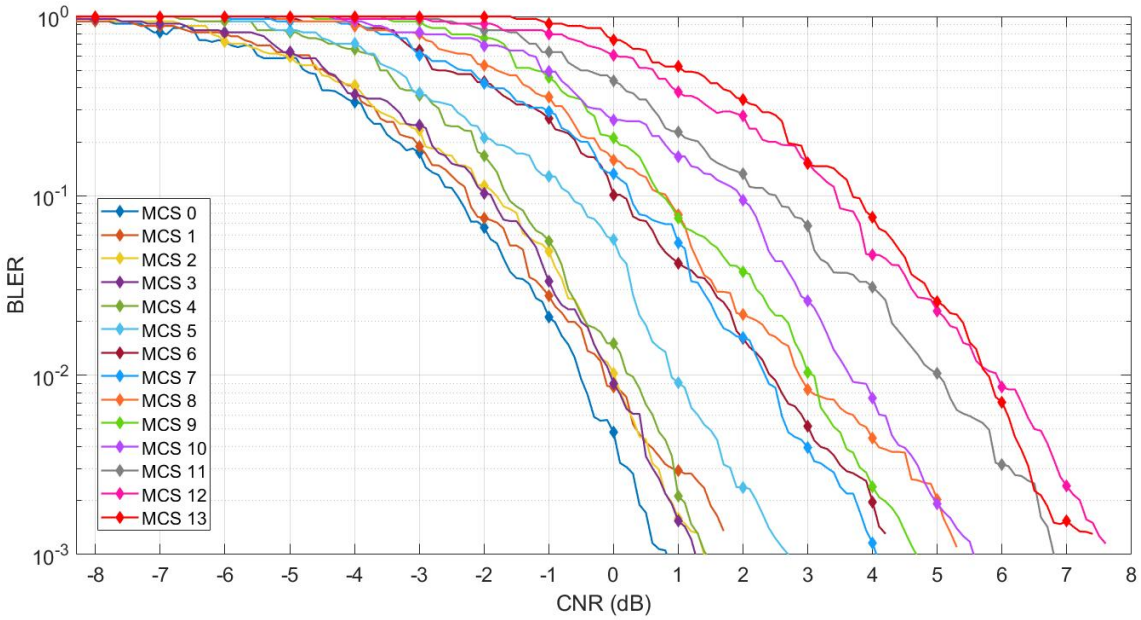

Figure 5.7: BLER v.s. CNR for 64 repetitions and DS=300ns.

We observe a similar example with the same parameter of Doppler frequency shift and the same stopping condition, while changing the number of repetitions to 64 repetitions and increasing the delay spread to 300 ns, as shown in the Figure 5.7. Once again we can deduce that increasing the MCS results in higher CNR needed to obtain the same BLER. In the beginning of the simulations, for high values of BLER, each MCS curve follows a similar slope, with the curve of MCS 0 starting to drop first, followed by the rest as the order increases. After BLER of 10% some of the curves start to intersect and higher order MCSs experience the same BLER for a lower CNR value in comparison

with lower order MCSs. For example, in the case of BLER = 0.3% MCS 3 shows lower value of CNR (0.6 dB) compared with MCS 2 (0.7 dB) and even MCS 1 (1.0 dB). For CNR = 1.0 dB, MCS 3 halves the BLER value (from 0.3% to 0.15%) compared to MCS 1 which holds the value of 0.3%.

A rather interesting gap between the curves of MCS 5 and MCS 6 can be noticed on the graph. Even though the TBS increases with each increase in order of the MCS, the gap between these two MCSs can be explained not only with more information bits processed, but as a result of the rate matching process. In the case of MCS 5 and lower, during the rate matching process some bits are repeated in order to match the output length. At the receiver side during rate recovery these bits are used to strengthen the LLR values. For this reason, we can assume that lower order MCSs will present better results. However from MCS 6 and higher, after the convolutional encoder we consider three bit streams that together present length larger than the supposed output length of the rate matching block. Therefore, the process of bit puncturing removes some of the bits. This influences the rate recovery at the receiver side and weakens the LLR values. For this reason, we may suppose that the gap has presented between the two MCSs due to the different behavior exhibited in the rate matching block.

As we increase the number of repetitions once again, but decrease the DS, keeping the other parameters and conditions the same, we plot a graph as depicted on the Figure 5.8.

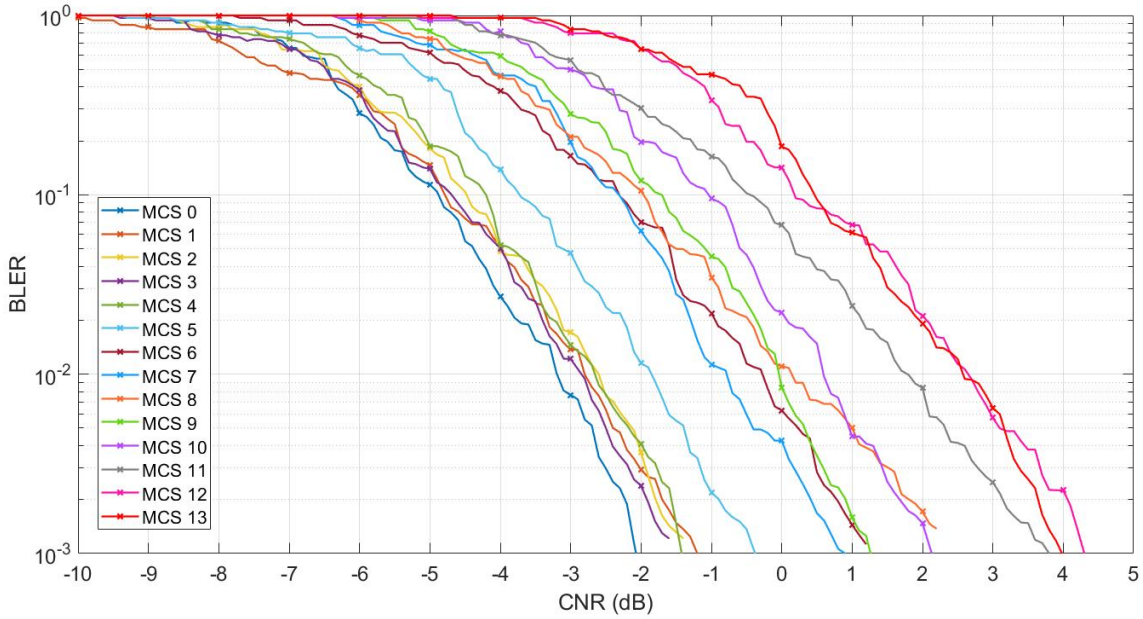

Figure 5.8: BLER v.s. CNR for 128 repetitions and DS=100ns.

The curves present confirm the previous statements regarding the increase of CNR as we increase the MCS, and produce once again the gap between the MCSs, placing the obtained minimal CNR values for BLER = 0.1% under 0 dB for the MCSs with the order lower than 5. This means that even when the signal strength is lower than the noise power, it is possible to decode the received signal. We underline that the same information has been sent 128 times in this example. The MCS 0 reaches the

BLER condition for CNR = -2.1 dB. At that CNR value, MCS 13 presents a BLER of 70%. This is a rather significat difference in performance of the two schemes. MCS 13 reaches the BLER condition at CNR = 4.0 dB. For the case of BLER = 1% MCS 0 needs CNR = -3.2 dB, while MCS 13 needs CNR = 2.6 dB. For the case of BLER = 10% MCS 0 needs CNR = -4.9 dB, while MCS 13 needs CNR = 0.5 dB. From these three examples we can follow how the width between the observed curves tends to increase (starting at 5.4 dB to 5.8 to 6.1 dB) and expect it would continue to do so as we pose stronger BLER condition.

Let us focus on the case of the set channel conditions (where the DS is equal to 10 ns and the Doppler frequency shift is 5 Hz) and follow the behavior of the system and the changes that occur only by increasing the number of repetitions for a specific set of MCSs. In the Figure 5.9, representing the four cases of repetition using 16, 32, 64 and 128 repetitions for the MCS 0 and 13, it can be seen that with each increase of the repetition number, the curve slope gets steeper. Thus, with the increase in the number of repetitions we reach the lower values of CNR faster. Either observing the blue colored lines marking MCS 0, or the red colored lines marking MCS 13, it is easily deduced that increasing the number of repetitions, the needed CNR to reach the BLER condition decreases i.e., the signal decoding conditions get better with each retransmission of the data bits.

In this case, using 128 repetitions with MCS 13 results in 0.1% BLER for CNR of 3.5 dB, while using 16 repetitions with MCS 0 the CNR value goes up to 5.9 dB. Hence we can observe that at the expense of longer processing time that is the product of increasing the repetitions number, we can send more data bits and achieve low BLER with low CNR values.

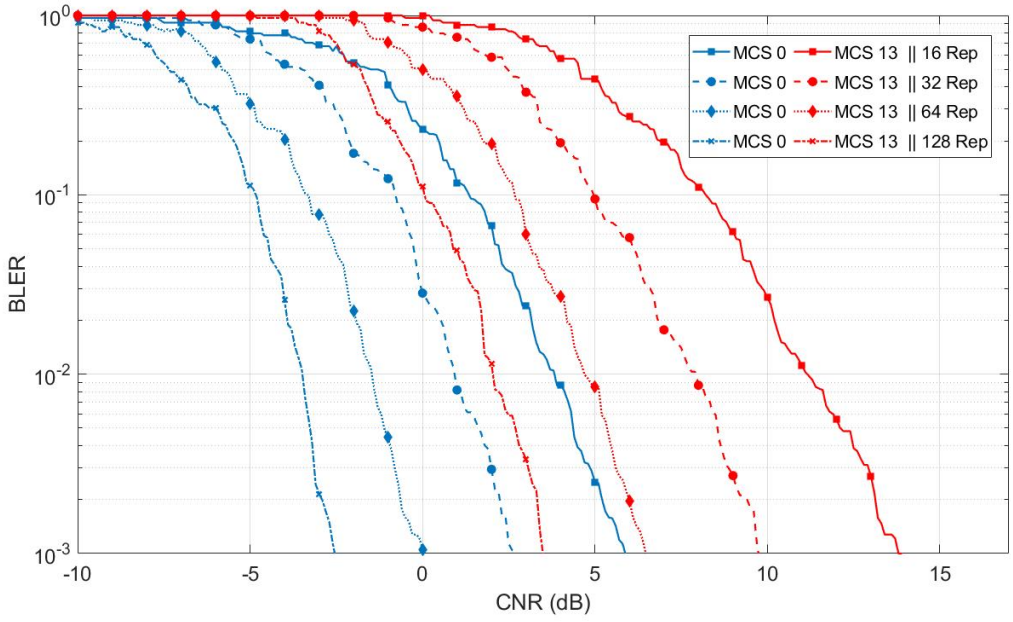

Figure 5.9: BLER v.s. CNR for DS=10ns and different repetition number.

The gain for each increase of repetition of about 3 dB in CNR is achieved, but for the first doubling of the repetition number (changing from 16 to 32) the gain is higher, and it decreases when the number

of repetitions gets higher (changing from 32 to 64 to 128). A deeper analysis is established by plotting the following graphs. We set the channel conditions by fixing the Doppler frequency shift to 5 Hz and the delay spread to 100 ns.

Figure 5.10 represents the minimal CNR value needed to achieve BLER of 0.1% per MCS for different cases of repeated transmissions, where the x-axis is used to represent the MCSs and the y-axis is used for the CNR values expressed in dB. This graph directly shows that we decrease the value of the needed CNR for the fixed condition of BLER as we increase the repetition number for each MCS used and we can easily measure it.

In order to focus on the difference between the minimal CNR values which is the gain that we get when doubling the number of repetitions, we plot the graph with the x-axis representing the MCSs and the y-axis representing the gain in dB, depicted in Figure 5.11. It can be gathered from analyzing the mentioned graph that even though there is always some gain when we double the number of repetitions, this gain is *(i)* not constant, *(ii)* decreases as number of repetitions increases for each MCS, but *(iii)* tends to increase with the increase in the order of MCS.

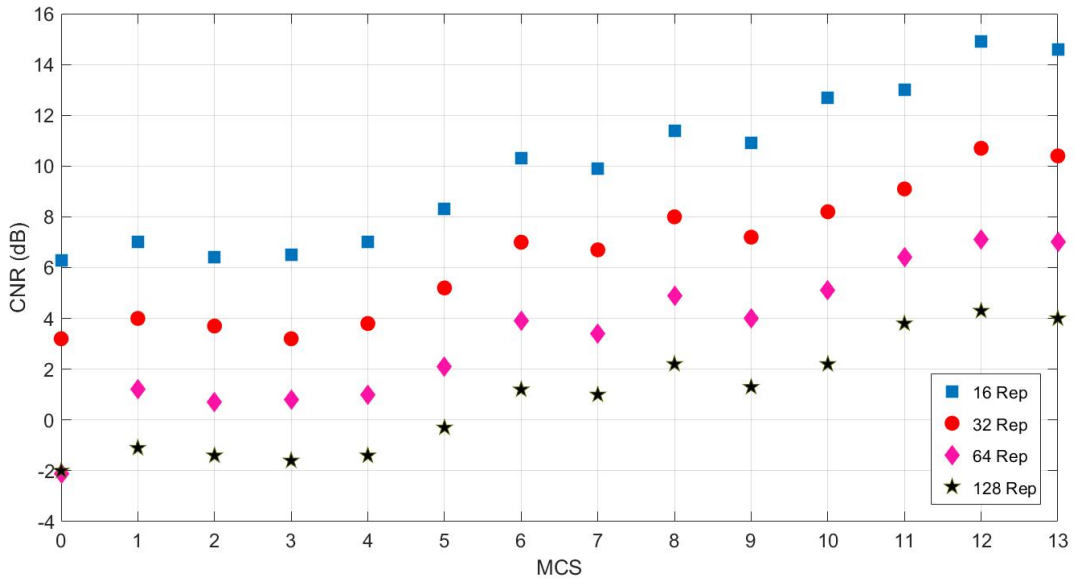

Figure 5.10: minCNR v.s. MCS for DS=100ns and different repetition numbers.

Apart from the number of repetitions, we assumed that the value of the delay spread would also affect the simulation results. The delay spread value is an important parameter considering the impact of multipath of a mobile communications channel. It can be defined as the difference in time between the arrival of the earliest component and the latest multipath component. As mentioned in Chapter 4, the CP duration for NB-IoT is 4.7 μs, hence the denormalized value of the DS cannot exceed this value. In the case it does, the Inter Symbolic Interference (ISI) developed between the OFDM symbols would make it impossible to decode the signal at the receiver side no matter how much we increase the signal power at the transmitter side. For this reason, we observe the worst case scenario of DS equal to 450 ns, that when denormalized gives the spread from TDL taps close to the value of the CP,

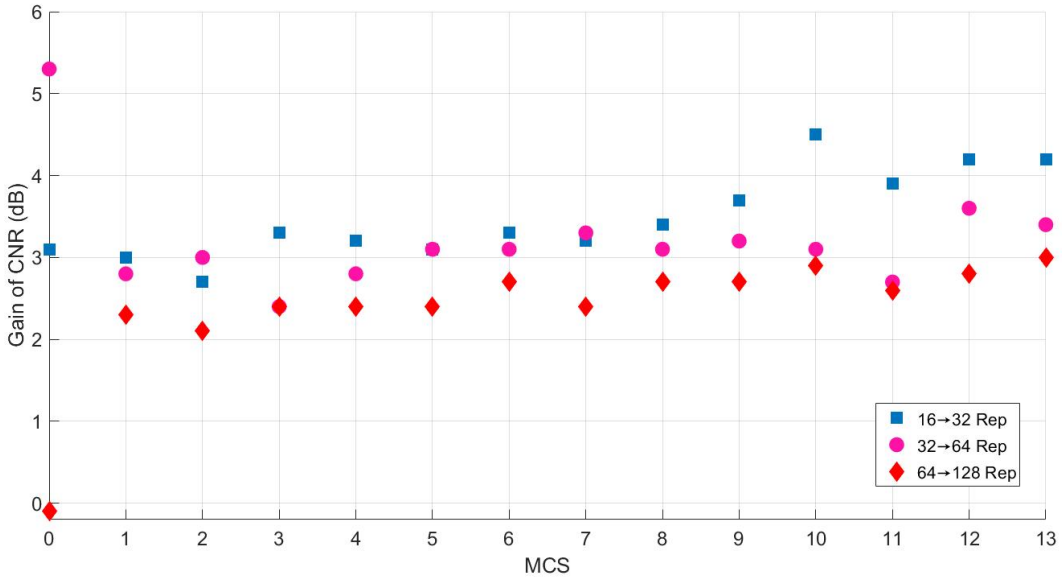

Figure 5.11: Gain in CNR v.s. MCS for DS=100ns and different repetition numbers.

depicted in the Figure 5.12. The value of the delay spread due to the last tap in the TDL-A model is equal to 4.3464 μs, considering the denormalization of the Table 5.2. The case of 64 repetitions is represented with the solid line, while the case of 128 repetitions is represented with the dash dotted line. Each color corresponds to a specific MCS. The plotted MCSs have been chosen randomly.

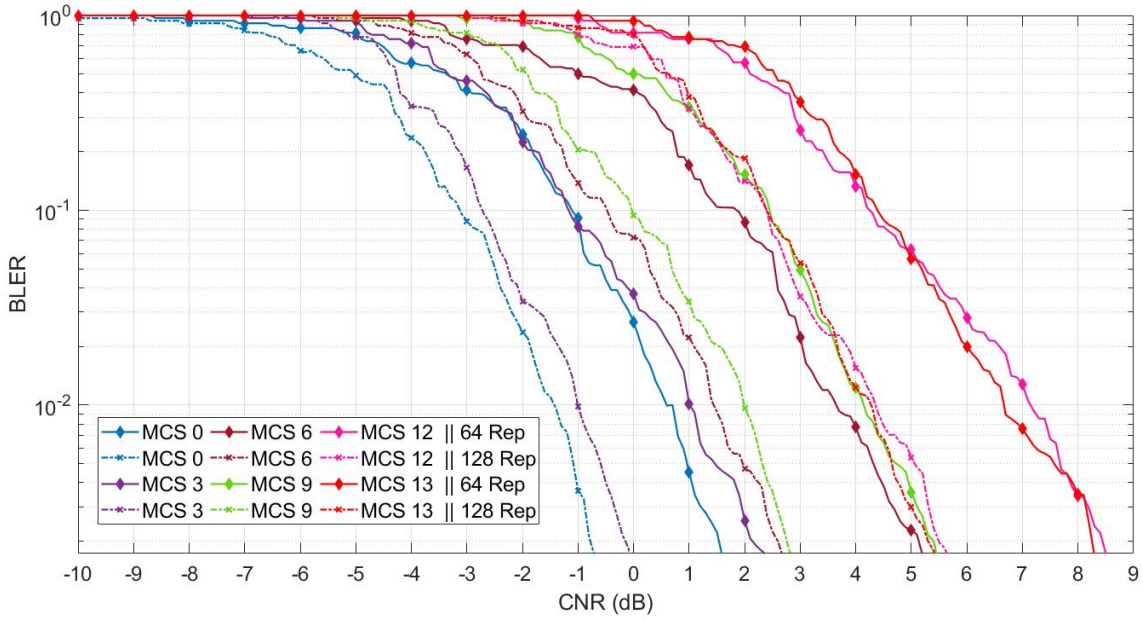

Figure 5.12: BLER v.s. CNR for DS=450ns and different MCS cases.

It can be observed from the graph that curves of the MCSs with close numbering tend to each other, like in this case MCS 0 and 3, MCS 6 and 9, MCS 12 and 13. This graph also shows that when

we increase the number of repetitions to 128 for MCS 12 and 13, the curves tend to follow the values of the MCS 6 and 9 in the case of 64 repetitions. In case we set CNR value to 2 dB and impose the condition of BLER lower than 1 % instead of using MCS 0 and 64 repetitions, we can increase the number of repetitions to 128 and use MCS 9. With the MCS 0 and 64 Repetitions, we are sending 16 information bits using 64 subframes with a duration of 1 ms per subframe. With the MCS 9 and 128 repetitions, we are sending 136 information bits using 128 subframes, again with the duration of 1 ms per subframe. Comparing these values, we get that the gain in spectral efficiency is increased 4.25 times when using the MCS 9 and 128 repetitions. Even though the increase in repetitions decreases the spectral efficiency, the gain from sending a higher number of bits prevails in this case.

In case we set CNR value at 4 dB, using 64 repetitions with MCS 9 the same BLER of 0.12% is reached in case of 128 repetitions and MCS 13. With the MCS 9 and 64 Repetitions, we are sending 136 information bits using 64 subframes with a duration of 1 ms per subframe. With the MCS 13 and 128 repetitions, we are sending 224 information bits using 128 subframes, again with the duration of 1 ms per subframe. Here, we have a reversed situation, since the decrease of the spectral efficiency due to the increase of repetitions is higher than the gain from sending more information bits, using MCS 9 and 64 repetitions gives 1.2143 times higher spectral efficiency. These examples show it is possible to fix the CNR value and the BLER condition, while adapting the MCS order and the repetition number, but we must take into account the effect these combinations have on the spectral efficiency as well.

We evaluate the effects of the change in delay spread for the MCS 8 in case of 64 and 128 repetitions, as depicted in the graphs (a) and (b) of the Figure 5.13 respectively. It can be noticed that as before, there is a gain in CNR when the number of repetitions is increased.

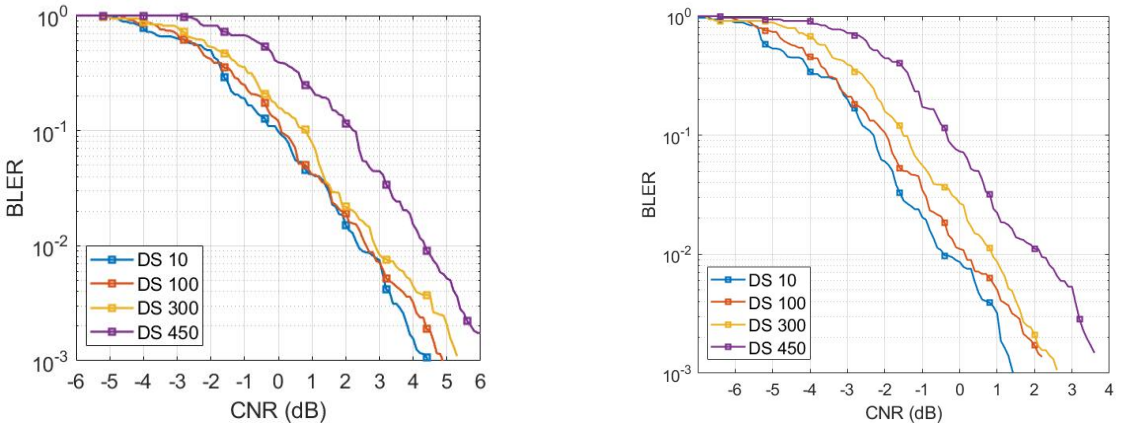

Figure 5.13: Comparison of different DS values for MCS 8 for 64 (a) and 128 (b) repetitions.

In both graphs, the curves of 10 ns DS and 100 ns DS are close together, followed by the 300 ns DS curve, while the 450 ns DS curve is farther away. We can, therefore, deduce that the delay spread does not impact the decoding of the signal so strongly as long as it is not close to the critical value, which coincides with the CP duration of the OFDM symbol. We can observe that the impact of the DS is more noticeable in the case (b) with the higher number of repetitions, showing that the longer we use

the channel the more its distortions in our transmissions are visible. However, taking into account that not all the taps induce the same delay spread and that the power produced by each tap varies as well, we can make an assumption that even if the channel conditions worsen, using more robust MCSs, we can even expect that our signal gets decoded, considering a high number of repetitions. For this reason in Figure 5.14 we examine the case of a DS equal to 1000 ns with 128 repetitions.

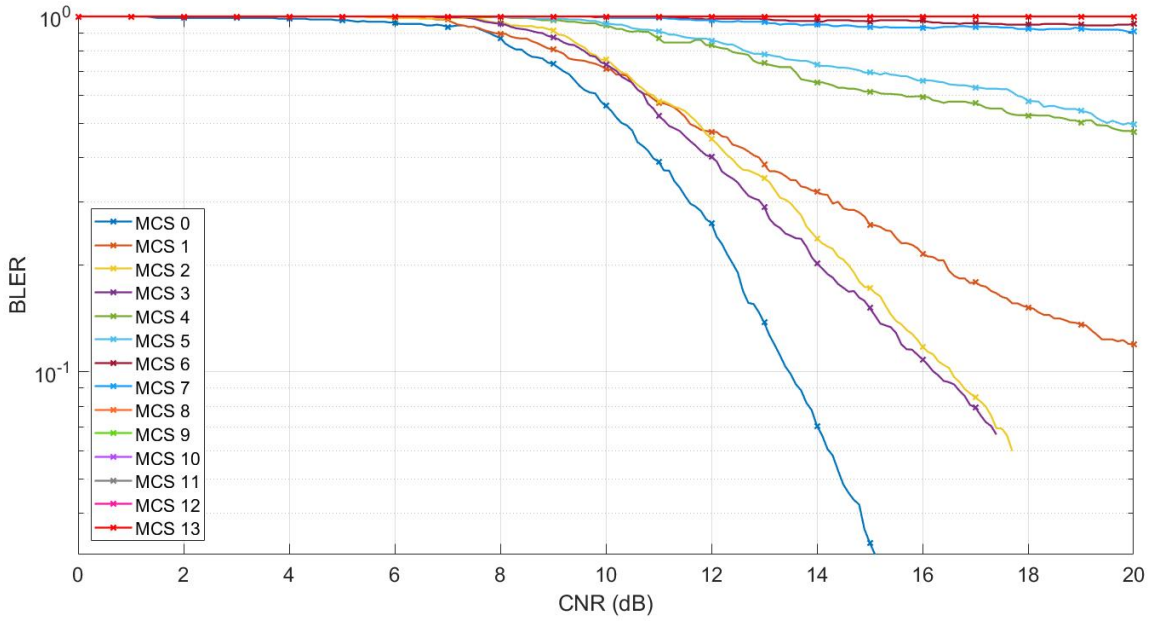

Figure 5.14: BLER v.s. CNR for DS=1000ns and different MCS cases.

This graph differs a lot compared to the previous values of CNR needed in the case of 128 repetitions and lower DS. We can see that only the first four MCS curves show a decrease, with MCS 0 being the only one to reach BLER = 1% for CNR = 15.1 dB. On the other hand, this is a very interesting result that shows us even in the presence of ISI caused by the delay spread of some taps being close to or even larger (for taps 20, 21, 22 and 23) than the CP duration, with high enough CNR, high number of repetitions and a low order MCS, decoding of the sent bits is possible.

The past results have taken into account only the stand-alone mode. In the Figure 5.15 we examine the case of in-band operation mode with 32 repetitions, DS of 100 ns and a Doppler frequency shift of 5 Hz. The maximum order of the MCS is 11, due to the fact that the first 3 OFDM symbols in the frame are not used for storing the data bits. Moreover, this mode uses in total 16 reference signals, 8 NRS and 8 CRS, unlike the stand-alone mode which does not contain CRS. Therefore we can expect better channel estimation per subframe, meaning that the repetition number does not need to be as high as in the case of stand-alone.

The condition of BLER smaller than 0.1% is reached for all the MCSs for a CNR value lower than 4 dB. The lowest value of CNR = -2.4 dB is obtained with MCS 1, while the highest value of CNR = 3.5 dB is obtained with MCS 11. The curves present rather a gentle slope. Schemes from 0 to 5 reach the BLER condition for CNR values below the noise. The rest at CNR = 0 dB present the

following BLER: MCS 6 0.5%, MCS 7 0.7%, MCS 8 1.1%, MCS 9 0.9%, MCS 10 1.5% and MCS 11 4.6%. Overall, at CNR = 0 dB, all of the MCSs present BLER smaller than 5% meaning that out of 30.000 evaluated subframes less than 1.500 are erroneous.

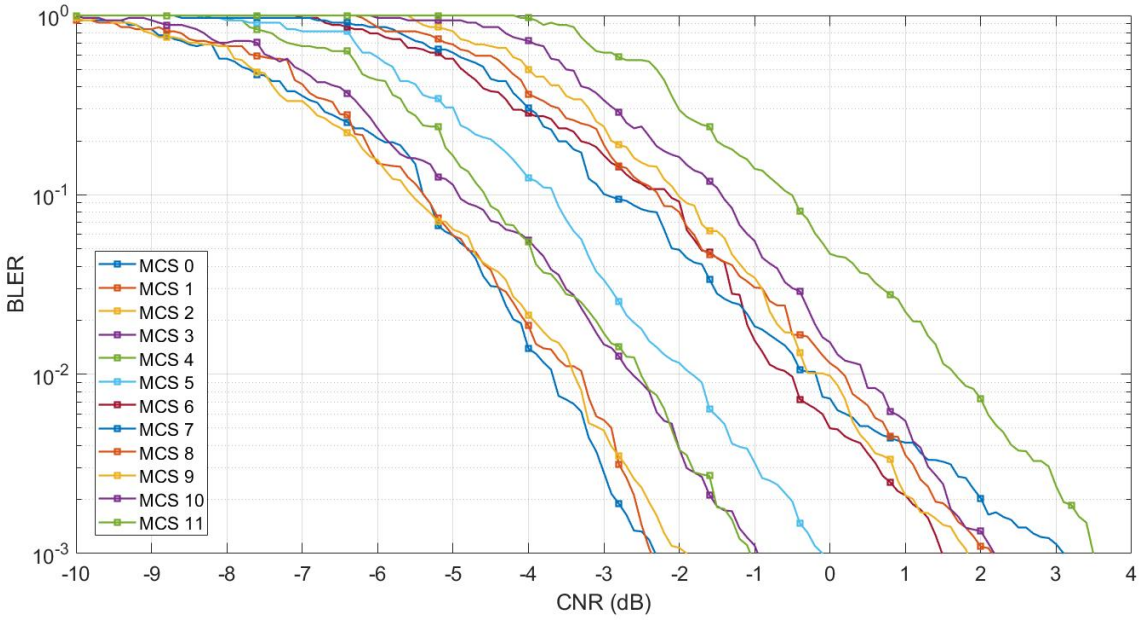

Figure 5.15: BLER v.s. CNR for DS=100ns and different MCS cases, in-band mode.

In the Figure 5.16 we plot the two cases of operation modes where the DS is set to 100 ns.

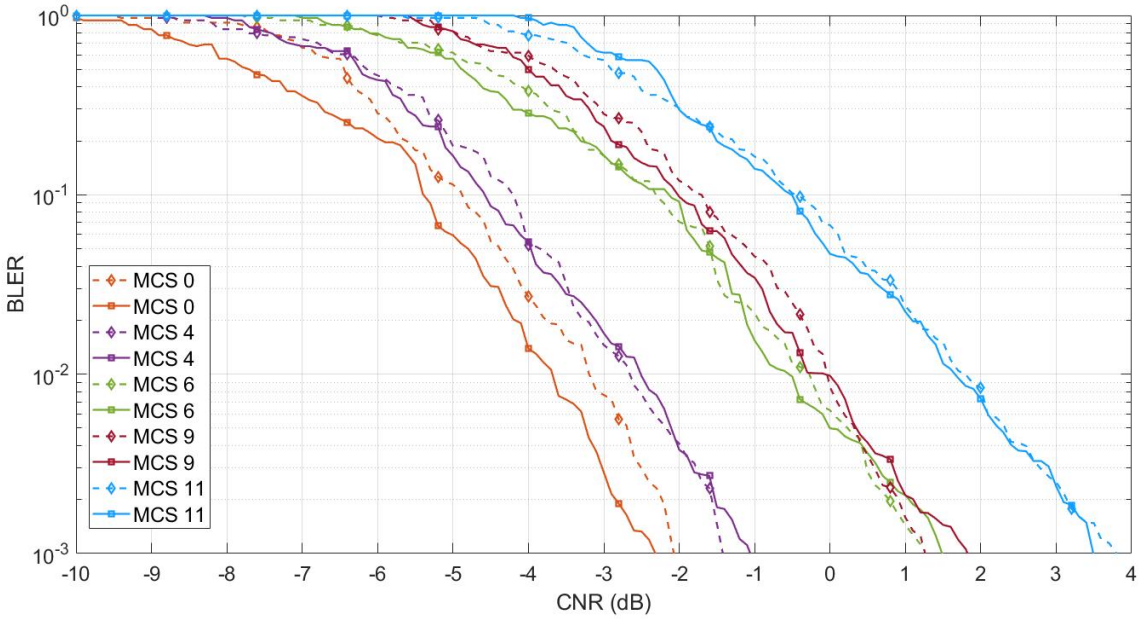

Figure 5.16: BLER v.s. CNR for DS=100ns and different MCS cases, in-band mode vs. stand-alone mode.

The in-band mode with 32 repetitions is represented with the full line and the stand-alone mode

with 128 repetitions is represented with the dotted line. The case of 128 repetitions was chosen due to the fact it presented similar results regarding the minimal CNR as previously mentioned in-band mode case, as these results have already been discussed with Figure 5.8. The MCSs have been chosen randomly.

This graph confirms the assumption of similar behavior of one MCS in the two different operation modes (each characterized with a different repetition number). We can see that only for the case of MCS 0 we have a slight difference between the curves, while for the higher order MCSs the curves tend to intersect multiple times. Based on this, we can conclude that the gain we get from increasing the number of repetitions 4 times in stand-alone mode is almost the same as the gain we get from switching from stand-alone to in-band mode. Due to the higher number of reference signals, in-band mode shows better channel estimation performance, at the expense of a smaller number of REs available for data bits. However, in-band mode does not require high number of repetitions, and for the same TBS offers better results than the stand-alone mode.

Guard-band mode has not been evaluated in this work since it presents the same frame structure as the stand-alone mode.

Chapter 6

Conclusions and future work

6.1 Conclusions

In this work we have examined the physical layer characteristics of the NB-IoT standard as defined in the 3GPP recommendations. The most important conclusions derived from everything that has been developed in this thesis are the following:

- The introduction of the process of repetition strengthens the values of channel estimation, resulting in a lower CNR i.e., signal power needed at the transmitter side. As the increase in the order of MCSs decreases the CNR, with the appropriate combination of a high order MCS and a high repetition number, we can balance the spectral efficiency gain/loss with the provided CNR, whilst maintaining the same BLER.
- The gain obtained from increasing the number of repetitions is not constant, but decreases with each doubling of the repetition number compared to the previous value. However, it shows higher values for high order MCSs compared to the low order MCSs.
- The channel conditions do not pose a loss higher than 3 dB in CNR as long as the values of the delay spread are close to the CP duration. Although, even in poor, highly non-ideal channel conditions it is possible to decode the signal, low order MCS and a high number of repetitions is necessary.
- The additional reference signals found in in-band mode compensate for the high number of repetitions in the stand-alone case, meaning in-band mode offers lower CNR values compared to the stand-alone mode for the same MCS and number of repetitions.

6.2 Future work

As NB-IoT is a technology constantly being enhanced and improved, the built simulator will need the adequate upgrades as new releases come out. The performance of higher order MCSs can be evaluated by implementing the 16QAM modulation method. The simulator could be adapted for the uplink version i.e., the NPUSCH. This would involve SC-FDMA instead of OFDM, turbo coding instead of convolutional coding, an additional SCS of 3.75 kHz and the implementation of single-tone transmission mode.

Rel-17 introduced the first steps towards NTN integration in the 5G communication systems. NTN networks offer a wide variety of solutions and support for the existing terrestrial networks. As far as massive IoT and NB-IoT are concerned, an interesting example would be a maritime scenario of tracking and enabling communication in areas which can not be reached with the current terrestrial systems. The physical layer performance could further be evaluated by implementing a new channel model inside the simulator. In the 3GPP technical report [23] the NTN channel model is defined as a variation of the TDL channel following Rayleigh distribution with a lower number of taps. However, due to the addition of another component in the transmission chain, we get additional parameters that affect the channel model and enhanced effects of some other parameters (such as the Doppler frequency shift, whose influence increases compared to the terrestrial TDL channel model). This channel model would need calibration.

As the technologies evolve and become more complex, new challenges in computer simulations arise. At a certain point traditional software tools and hardware limitations will constrain the scope of simulators. A new approach has been introduced with Sionna, an open-source library written in python for physical layer research. It enables rapid prototyping, benchmarking against state of the art, realistic industry-grade evaluations, native support of neural networks, and reproducibility. [24] The transition to an open-source library would not only be beneficial for the researcher, but also for the entire community as it would allow experts in different areas to share their ideas and research. In this way researchers could focus on improving one specific part of the end-to-end communication systems, without dissipating time implementing auxiliary components.

Bibliography

[1] L. Rosencrance, *3 NB-IoT use cases bring advantages and challenges*, https://www.techtarget.com/iotagenda NB-IoT-use-cases-bring-advantages-and-challenges, Accessed in July, 2022.

[2] A. Zaidi, Y. Hussain, M. Hogan, and C. Kuhlins, "Cellular IoT Evolution for Industry Digitalization," Ericsson, Tech. Rep., 2019.

[3] iNGENIOUS project, *Deliverable 3.1 - Communication of IoT Devices*, 2021.

[4] Y. Li, X. Cheng, Y. Cao, D. Wang, and L. Yang, "Smart Choice for the Smart Grid: Narrowband Internet of Things (NB-IoT)," *IEEE Internet of Things Journal*, vol. 5, no. 3, pp. 1505–1515, 2018.

[5] ITU-R, "Report M.2412-0, Guidelines for evaluation of radio interference technology for IMT-2020," ITU, Tech. Rep., 2017.

[6] ITU, *Emerging Trends in 5G/IMT2020*, 2016.

[7] E. Rastogi, N. Saxena, A. Roy, and D. R. Shin, "Narrowband Internet of Things: A Comprehensive Study," *Computer Networks*, vol. 173, no. 107209, 2020.

[8] 3GPP, "TS 36.300 - Technical Specification LTE; Evolved Universal Terrestrial Radio Access (E-UTRA) and Evolved Universal Terrestrial Radio Access Network (E-UTRAN); Overall Description; Stage 2 (Release 13)," 3GPP, Tech. Rep., 2016.

[9] 3GPP, "TS 36.300 - Technical Specification LTE; Evolved Universal Terrestrial Radio Access (E-UTRA) and Evolved Universal Terrestrial Radio Access Network (E-UTRAN); Overall Description; Stage 2 (Release 14)," 3GPP, Tech. Rep., 2017.

[10] 3GPP, "TS 36.300 - Technical Specification LTE; Evolved Universal Terrestrial Radio Access (E-UTRA) and Evolved Universal Terrestrial Radio Access Network (E-UTRAN); Overall Description; Stage 2 (Release 15)," 3GPP, Tech. Rep., 2018.

[11] 3GPP, "TS 36.300 - Technical Specification LTE; Evolved Universal Terrestrial Radio Access (E-UTRA) and Evolved Universal Terrestrial Radio Access Network (E-UTRAN); Overall Description; Stage 2 (Release 16)," 3GPP, Tech. Rep., 2020.

[12] 3GPP, "TS 36.300 - Technical Specification LTE; Evolved Universal Terrestrial Radio Access (E-UTRA) and Evolved Universal Terrestrial Radio Access Network (E-UTRAN); Overall Description; Stage 2 (Release 17)," 3GPP, Tech. Rep., 2021.

[13] 3GPP, "TS 36.211 - Technical Specification LTE; Evolved Universal Terrestrial Radio Access (E-UTRA); Physical channels and modulation (Release 17)," 3GPP, Tech. Rep., 2021.

[14] *ShareTechNote*, http://www.sharetechnote.com/, Accessed in July, 2022.

[15] *5G LTE Narrowband Internet of Things (NB-IoT)*. CRC Press, 2019.

[16] M. Kanj, M. L. Guen, and V. Savaux, "A Tutorial on NB-IoT Physical Layer Design," *IEEE Communications Surveys and Tutorials*, 2020.

[17] Y.-P. E. Wang, A. A. X. Lin, A. Grovlen, *et al.*, "A primer on 3GPP Narrowband Internet of Things," *IEEE Commun. Mag.*, vol. 55, no. 3, pp. 117–123, 2017.

[18] 3GPP, "TS 36.213 - Technical Specification LTE; Evolved Universal Terrestrial Radio Access (E-UTRA); Physical layer procedures (Release 17)," 3GPP, Tech. Rep., 2021.

[19] 3GPP, "TS 36.212 - Technical Specification LTE; Evolved Universal Terrestrial Radio Access (E-UTRA); Multiplexing and channel coding (Release 17)," 3GPP, Tech. Rep., 2021.

[20] J. Schlienz and D. Raddino, "Narrowband Internet of Things Whitepaper," Rhode and Schwarz, Tech. Rep., 2016.

[21] 3GPP, "TS 36.211 - Technical Specification LTE; Evolved Universal Terrestrial Radio Access (E-UTRA); Physical channels and modulation (Release 16)," 3GPP, Tech. Rep., 2020.

[22] ETSI, "TR 38.901 - 5G; Study on channel model for frequencies from 0.5 to 100 GHz (Release 17)," ETSI, Tech. Rep., 2022.

[23] 3GPP, "Study on New Radio (NR) to support non-terrestrial networks," 3GPP, Tech. Rep., 2019.

[24] J. Hoydis, S. Cammerer, F. A. Aoudia, *et al.*, *Sionna: An Open-Source Library for Next-Generation Physical Layer Research*, 2022.